Study on the Magnetoelectric Effect in Magnetic Oxides

Eiji KITA

OSAKA UNIVERSITY
GRADUATE SCHOOL OF ENGINEERING SCIENCE
DEPARTMENT OF MATERIAL PHYSICS
TOYONAKA OSAKA

Study on the Magnetoelectric Effect in Magnetic Oxides

Eiji KITA

Abstract

Magnetoelectric (ME) effect in two oxides was investigated. One was an antiferromagnet, Cr_2O_3, and the other was a ferrimagnet Fe_3O_4.

To study atomic mechanisms, electric shift of the antiferromagnetic resonance (AFMR) as well as precise measurements of the ME effect was performed in Cr_2O_3. The use of a SQUID magnetometer in a measurement of ME susceptibilities (α) of Cr_2O_3 from 1.6 to 270 K was reported. The sensitivity of the magnetometer was about 10^{-8} emu. A static measurement sweeping the applied electric field provided an easy method to confirm the sign and the linearity of the response. The characterizing values of α were determined and δg at 4.2 K was deduced from $\alpha_{//4.2K}$: $\delta g = -3.5 \times 10^{-8}$ at E = 1 kV/cm after the parallel ME cooling. An unusual temperature dependence of α discovered in a crystal was also reported.
The shift caused by the electric field parallel to the c axis in the AFMR of Cr_2O_3 was successfully carried out at 4.2 K by the use of ac electric field modulation method at the frequency of 24.2 GHz (low frequency mode). δD was evaluated as -1.1×10^{-6} cm^{-1} at E = 1 kV/cm. This magnitude was about 1/10 of that of Cr^{3+} in ruby.

ME effect at 77 K confirmed that the magnetic crystal symmetry of the low temperature phase of Fe_3O_4 is triclinic but the breaking of the mirror symmetry parallel to the $(1\bar{1}0)$ plane is very small. Anisotropy and external magnetic field dependence of the ME effect in Fe_3O_4 was measured and analyzed. It was disclosed that the tilting of the magnetization, due to the change of the magnetic anisotropy by the application of the electric field, is a dominant

mechanism, though the existence of the non-tilting mechanism could not be excluded. The main part of the magnetic anisotropy accompanied by electric polarization, which has mirror symmetry parallel to the $\underline{b}$ plane, was analyzed by spherical harmonics up to the fourth order. This polarization dependent part was much smaller than the total magnetic anisotropy energy. Direction of the spontaneous electric polarization was estimated as - 15° from [111] or + 19° from $[\bar{1}\bar{1}2]$ within the $\underline{b}$ plane. Dispersion of the ME effect, relaxation time of which was approximately 2 μsec, and the anisotropy in the efficiency of the direction of applied electric field was discovered and was attributed to the dispersion and the anisotropy of the electric susceptibility, on a preliminary measurement of the electric susceptibility. The structure of the low temperature phase was discussed briefly in connection with the model proposed by Mizoguchi.

CONTENTS

CHAPTER 1 INTRODUCTION

Classification of the 122 Shubnikov groups according to "magnetoelectric types"[17)]

Type of ordering		Permitted terms of stored free enthalpy	Shubnikov point groups	
Magnetic	Electric		V_a not permitted	V_a permitted
D	P	E EHH	$\boxed{1'}$, $\boxed{21'}$, $\boxed{m1'}$, $\boxed{mm21'}$, $41'$, $4mm1'$, $31'$, $3m1'$, $61'$, $6mm1'$	
$\bar{M}$	P	E HEE EHH	$6'$, $6'mm'$	
$\bar{M}$	P	E EH HEE EHH	$4'$, $4'mm'$	$\boxed{\bar{4}'m'2}$, $4mm$, $3m$, $6mm$
M	P	E H EH HEE EHH	$\boxed{\bar{6}'m'2}$, $3m'$, $4m'm'$, $6m'm'$	$\boxed{11'}$, $\boxed{\bar{1}'}$, 3, 4, 6, $\boxed{m'}$, $\boxed{2'}$, $\boxed{\bar{4}'}$, $\boxed{mm2'}$
M	P	H EH HEE EHH	3, $32'm'$	$\boxed{3'2'2}$, $42'2'$, $32'$, $62'2'$
M	P	H HEE EHH	$\bar{6}$, $\bar{6}m'2'$	
M	O	H HEE	$\boxed{\bar{1}}$, $\boxed{2/m}$, $\boxed{2'/m}$, $\boxed{m'm'm}$, $4/m$, $4/mm'm'$, 3, $3m'$, $6/m$, $6/mm'm'$	
$\bar{M}$	P	EH HEE EHH	222, 422, $\bar{4}2m$, $4'22'$, $\bar{4}'2m'$, 32, 622, $\bar{6}'m'2$, 23, $\bar{4}'3m'$	$3'$, $\bar{3}'2'm$, $\bar{6}'$, $\bar{6}'m2'$
$\bar{M}$	P	HEE EHH	$\bar{6}m2$, $6'2'2$	
$\bar{M}$	P	EH	$m'm'm'$, $4'/m'$, $4'/m'm'm$, $4'm'm'm'$, $3'm'$, $6'm'm'm'$, 432, $m'3$, $m'3m'$	$1'$, $2/m'$, $2'/m$, mmm', $4/m'$, $4/m'mm$, $3'$, $3'm$, $6'm'$, $6/m'mm$
$\bar{M}$	O	HEE	mmm, $4'/m$, $4mmm$, $4'/mmm'$, $6/mmm$ $3m$, $6'/m'$, $6'/m'm'm$, $m3$, $m3m'$	
$\bar{M}$	P		$4'32'$	
$\bar{M}$	P	EHH	$\bar{4}3m$	
D	P		$2221'$, $\bar{3}1'$, $4221'$, $\bar{4}2m1'$, $6221'$, $321'$, $\bar{6}1'$, $\bar{6}m21'$, $231'$, $\bar{4}3m1'$	
$\bar{M}$	O		$m3m$	
D	P		$4321'$	
$\bar{M}$	P		$6'/m$, $6'/mm'm$, $m'3m$	
D	O		$\bar{1}1'$, $2/m1'$, $mmm1'$, $4/m1'$, $4/mmm1'$, $\bar{3}1'$, $\bar{3}m1'$ $6/m1'$, $6/mmm1'$, $m31'$, $m3m1'$	

$\square$ "Weak ferromagnetism" (Dzialoshinsky 1957)[17] permitted, corresponding Shubnikov groups determined by Tavger[18] for nearly uniaxial antiferromagnets.

$\boxed{}$ "Weak ferroelectricity" permitted.

Type of order: M = pyro-, ferro-, or ferrimagnetic; P = pyro-, ferro-, or ferrielectric; $\bar{M}$ = antiferromagnetic; $\bar{P}$ = antiferroelectric or orthoelectric; D = diamagnetic, or paramagnetic, or antiferromagnetic; O = orthoelectric, or paraelectric, or antiferroelectric.

V_a = invariant velocity vector.[21,22]

H: spontaneous magnetization permitted; E: spontaneous polarization permitted; EH: linear magnetoelectric effect permitted; EHH: second-order magnetoelectric effect (I) ("paramagnetoelectric effect"),[19] piezoelectricity, Pockels effect, etc., permitted (see Table II); HEE: second-order magnetoelectric effect (I), piezomagnetism, "Mockels" effect,[20] etc., permitted (see Table I).

Electric and magnetic response of materials have been main problems in solid state physics and substances with spontaneous magnetic or electric polarization have been providing most usefull materials. Generally speaking, magnetic and electric polarization in a solid are considered to be independent: magnetic moment is a function of only a magnetic field and electric polarization is that of an electric field. In other words, the categories of ferromagnets and ferroelectrics were regarded as independent one and did not overlap. The interaction between the magnetic moment and the electric polarization, however, exists in some materials. In such materials, the magnetization can be induced by the electric field and electric polarization can be induced by the magnetic field. These phenomena are called magnetoelectric (ME) effect. Possibility of the linear ME effect, an appearance of the polarization proportional to the applied field, was proposed already in 1894, though the existence of this effect in a magnetically disordered material was rejected by Van Vleck in 1932.[1] The first correct prediction of linear ME effect was made in 1957 by Landau and Lifshitz[2] on the symmetry consideration for magnetically ordered crystals. Antiferromagnetic Cr_2O_3 was proposed as a candidate by Dzyaloshinski[3] in 1959 and was really observed by Astrov[4] and Folen et al.[5] in 1960. Since then, more than 30 materials have been found to show the linear ME effect. In recent years, higher order effect, quadratic in the electric and/or magnetic field, were discovered.

These effects depend on the magnetic symmetry of the crystal, which also affects other physical phenomena. The importance of I, inversion of space, in the dielectric properties of solid is well known. If a crystal has I as a symmetry element, the crystal can neither be pyroelectric nor piezoelectric. In the magnetic phenomena, there is another important symmetry operator, R, which expresses time reversal or the reversal of magnetization and magnetic field. The point group of the magnetic crystal should be augumented by this operator and be extended.

In this chapter, outline of the investigations on the ME effect is given and the purpose of the present study is described.

§ 1-1. Thermodynamic Potential and Magnetic Symmetry

In their famous text book, Landau and Lifshitz[2] discussed the thermodynamic potential of a material placed in uniform fields from the stand point of the symmetry of the crystal. When the external electric and the magnetic fields ($\vec{E}$ and $\vec{H}$) are not too strong and there are no spontaneous polarizations, free energy (F) of the material can be expanded in $\vec{E}$ and $\vec{H}$ as

$$\begin{aligned} F &= F_o + F^{ME} \\ &= -\frac{1}{2}\varepsilon_{ij}E_iE_j - \frac{1}{2}\chi_{ij}H_iH_j + \cdots\cdots \\ &\quad - \alpha_{ij}E_iH_j - \beta_{ijk}H_iE_jE_k - \gamma_{ijk}E_iH_jH_k - \partial_{ijkl}E_iE_jH_kH_l \\ &\quad + \cdots\cdots \quad . \end{aligned} \tag{1-1}$$

Here, F_o is the part of the free energy without cross terms of $\vec{E}$ and $\vec{H}$ and F^{ME} is the part of cross terms. Electric polarization ($\vec{P}$) is deduced by the relation $\vec{P} = -\partial F/\partial\vec{E}$ and magnetization ($\vec{M}$) is deduced from $\vec{M} = -\partial F/\partial\vec{H}$.

$$P_i = \varepsilon_{ij}E_j + \alpha_{ij}H_j + \beta_{ijk}H_jE_k + \gamma_{ijk}H_jH_k + \cdots \tag{1-2a}$$

$$M_i = \chi_{ij}H_j + \alpha_{ij}E_j + \beta_{ijk}E_jE_k + \gamma_{ijk}E_jH_k + \cdots . \tag{1-2b}$$

Here, ε_{ij} is the electric and χ_{ij} is the magnetic susceptibility tensor. α_{ij} is the linear ME susceptibility tensor, β_{ijk} and γ_{ijk} are the second order ME susceptibility tensors and ∂_{ijkl} is the third order ME susceptibility. The problem is the property of these tensors which determines the ME response of the material.

Physical properties of the crystal are closely related to the symmetry of it. The response to the applied uniform field, or the form of susceptibility tensors, is determined by the point symmetry

of the crystal. Consider the case of the linear response, for a time. A property tensor ($\tilde{A}$) expresses the relation between a physical quantity ($\vec{Y}$) and an applied field ($\vec{X}$):

$$\vec{Y} = \tilde{A} \cdot \vec{X} \ . \tag{1-3}$$

When the crystal has a symmetry operator U, eq.(1-3) must be invariant to the operation,

$$U \cdot \vec{Y} = \tilde{A} \cdot (U \cdot \vec{X}) = U \cdot (\tilde{A} \cdot \vec{X}). \tag{1-4}$$

Then,

$$\tilde{A} = U^{-1} \cdot \tilde{A} \cdot U. \tag{1-5}$$

This condition should be satisfied for all the symmetry operators.

In the case of the ME effect, it should be noted that $\vec{Y}$ is an axial vector when $\vec{X}$ is a polar vector or vice versa. Inversion I and time reversal R play special role in such a case. According to eq.(1-2), the linear ME effect is expressed as

$$P_i = \alpha_{ij} H_j , \tag{1-6a}$$

$$M_i = \alpha_{ij} E_j , \tag{1-6b}$$

and

i) when R is a symmetry element of the crystal,

$$R \vec{E} = \vec{E},$$

$$R \vec{M} = - \vec{M},$$

and eq.(1-4) leads to

$$-\vec{M} = \alpha\vec{E} \quad (= \vec{M}).$$

Then, $\tilde{\alpha} = -\tilde{\alpha}$, and $\tilde{\alpha} \equiv 0$: no linear ME effect is expected in paramagnetic or diamagnetic materials. This was the point made by Van Vleck.

ii) When I is a symmetry element of the crystal,

$$I\vec{E} = -\vec{E},$$

$$I\vec{M} = \vec{M}.$$

and eq.(1-4) leads to

$$\vec{M} = -\alpha\vec{E} \quad (= \alpha\vec{E}).$$

Then, $\tilde{\alpha} = -\tilde{\alpha}$, and $\tilde{\alpha} \equiv 0$: a crystal with inversion can not show the linear ME effect. It is noted that the magnetic material with the spontaneous magnetization and linear ME effect can not possess inversion as a crystal symmetry.[6)]

The symmetry of property tensors of materials is determined by the point group of the crystal. There are 32 classical crystal classes augmented by 90 magnetic crystal classes: 122 crystal classes in total.[7)] It was verified that linear ME effect exists in 58 of 90 magnetic crystal classes and their tensor form were divided into 11 different types.[6)] They are shown in Table 1-I with examples. About thirty materials have been found to show the linear ME effect. The list of them was given in several review articles.[6,8,9)]

Naturally, crystals with the same atomic structure can be different in the ME properties when the magnetic structure is different. For example, Cr_2O_3, αFe_2O_3 and αAl_2O_3 are isomorphous in the atomic structure but are different in magnetic structure.

Table 1-I. Magnetic crystal class and ME tensor $\tilde{\alpha}$ with an example.

Magnetic crystal class	ME tensor	Example	Symmetry	
1, $\bar{1}'$	$\begin{matrix}\alpha_{11} & \alpha_{12} & \alpha_{13}\\ \alpha_{21} & \alpha_{22} & \alpha_{23}\\ \alpha_{31} & \alpha_{32} & \alpha_{33}\end{matrix}$	Fe_3O_4 [10]	1	
2, m' 2/m'	$\begin{matrix}\alpha_{11} & \alpha_{12} & 0\\ \alpha_{21} & \alpha_{22} & 0\\ 0 & 0 & \alpha_{33}\end{matrix}$	DyOOH [11]	2/m'	α_p† $= 9.8 \times 10^{-5}$
2', m, 2'/m	$\begin{matrix}0 & 0 & \alpha_{13}\\ 0 & 0 & \alpha_{23}\\ \alpha_{31} & \alpha_{32} & 0\end{matrix}$	ErOOH [12]	2'/m	α_p† $= 4.5 \times 10^{-4}$
222, m'm'2, m'm'm'	$\begin{matrix}\alpha_{11} & 0 & 0\\ 0 & \alpha_{22} & 0\\ 0 & 0 & \alpha_{33}\end{matrix}$	$TbAlO_3$ [13]	m'm'm'	$\alpha_{11} = 2.2 \times 10^{-3}$
22'2', mm2*, m'm2', m'mm	$\begin{matrix}0 & 0 & 0\\ 0 & 0 & \alpha_{23}\\ 0 & \alpha_{32} & 0\end{matrix}$	$LiFePO_4$ [14]	m'mm	$\alpha_{32} = 1.0 \times 10^{-4}$
4, $\bar{4}'$, 4/m', 3, $\bar{3}'$, 6, $\bar{6}$, 6/m'	$\begin{matrix}\alpha_{11} & \alpha_{12} & 0\\ -\alpha_{12} & \alpha_{11} & 0\\ 0 & 0 & \alpha_{33}\end{matrix}$			
4', $\bar{4}$, 4'/m'	$\begin{matrix}\alpha_{11} & \alpha_{12} & 0\\ \alpha_{12} & -\alpha_{11} & 0\\ 0 & 0 & 0\end{matrix}$			
422, 4m'm', $\bar{4}'$2m', 4m'm'm', 32, 3m', $\bar{3}'$m', 622, 6m'm', $\bar{6}'$m'2, 6/m'm'm'	$\begin{matrix}\alpha_{11} & 0 & 0\\ 0 & \alpha_{11} & 0\\ 0 & 0 & \alpha_{33}\end{matrix}$	Cr_2O_3 [15]	$\bar{3}'$m'	$\alpha_{33} = 1.2 \times 10^{-4}$
4'22, 4mm', $\bar{4}$2m, $\bar{4}$2'm', 4'/m'mm'	$\begin{matrix}\alpha_{11} & 0 & 0\\ 0 & -\alpha_{11} & 0\\ 0 & 0 & 0\end{matrix}$	$DyPO_4$ [16]	4'/m'mm'	$\alpha_{11} = 1.2 \times 10^{-3}$
42'2', 4mm, $\bar{4}'$2'm, 4/m'mm, 32', 3m, $\bar{3}'$m, 62'2, 6mm, $\bar{6}'$m2', 6/m'mm	$\begin{matrix}0 & \alpha_{12} & 0\\ -\alpha_{12} & 0 & 0\\ 0 & 0 & 0\end{matrix}$			
2m, m'3, 432, $\bar{4}'$3m', m'3m'	$\begin{matrix}\alpha_{11} & 0 & 0\\ 0 & \alpha_{11} & 0\\ 0 & 0 & \alpha_{11}\end{matrix}$			

* α_{12} and α_{21} are non-vanishing elements instead of α_{23} and α_{32}.

† α_p is the value measured for a polycrystalline sample.

Cr_2O_3 has IR, αFe_2O_3 has I and αAl_2O_3 has I and R as the symmetry operation and only Cr_2O_3 shows the linear ME effect in the antiferromagnetic state. Even in a crystal of high symmetry in its atomic structure, ME effect can exist when the symmetry of its magnetic structure is low. Materials with triangular or conical spin structure such as $CuCr_2O_4$ or $MnCr_2O_4$ are expected to be ME materials. It is also to be noted that the magnetic symmetry of a ferromagnet is dependent on the spin axis which can be changed by the external magnetic field (see chapter 3).

The same sort of considerations can be adopted to the higher order ME effect, corresponding to the terms βHEE, $\gamma \dot{E}HH$ or $\partial EEHH$ in eq.(1-1).[17] If R exists, all elements of tensor β must be zero and if I exists, all elements of tensor γ must be zero. On the contrary, tensor ∂ exists in all cases but the magnitude is not detectable, in usual cases. When the crystal is spontaneously polarized, electric or magnetic, the crystal lacks I or R. The second order ME effect was really observed in such cases: β was found in the garnet family[18] (YIG,[19] GdIG,[20] DyIG[21]) and γ was found in the piezoelectric paramagnetic crystal $NiSO_4 \cdot 6H_2O$.[22]

§ 1-2. Experimental method of the ME effect measurement.

From eq.(1-2), it is clear that there are two alternative ways to determine the ME susceptibility tensor. In one way, the magnetization induced by the applied electric field is detected. In the other way, the electric polarization induced by the applied magnetic field is detected. In practice, the magnitude of the signal is so small that

high sensitive detector and/or high applied field is necessary. The magnitude of α is typically in the order of $10^{-3} \sim 10^{-6}$ in Gauss unit. (See Table 1-I.) (In Gauss unit, α is expressed by a dimensionless number.) Practically, measuring method of the linear ME effect may be divided into three groups.

a) ac method: induced magnetization[4,5] or electric polarization[23] by applied ac field is detected as output of a pick up coil or of electrodes. The frequency of the applied field is usually $1 \sim 100$kHz. The signal increases proportionally to the frequency, setting the lower limit of ω, but the spurious output leaked directly from input to the pick up system is proportional to ω^2 [24] and sets the higher limit of ω, though much effort have been attempted to suppress the coupling. Lock-in amplifier is usually used to eliminate the noise.

b) dc method; induced polarization by statically applied field is detected by a high sensitive magnetometer (astatic magnetometer[25] or SQUID magnetometer[26]) or an electrometer.[27] Back ground leakage is negligible in this case but the output is so small that the high applied field and the high sensitivity of the detector are necessary. Available magnetic field is much higher than the electric field and, in this sense, the detection of the electric polarization due to the applied magnetic field is easier, if the input impedance of the detector is high enough. However, the static measurement of absolute value of the electric polarization is not easy. Precise measurement is not expected when the resistivity of the sample is not high. On the other hand, the electrometer must have higher impedance

than the resistance of the sample.

c) Pulse method: induced polarization by pulsed field is detected.[28]

It is to be noted that the measurement of the absolute value of α, or the calibration of the detecting system, is much easier for the magnetic detection than the electric detection.

The higher order ME effect can be measured similarly to the linear effect by superposing dc biasing field, E_o or H_o, and ac modulating field, $E_1 \sin\omega t$ or $H_1 \sin\omega t$. The output at the frequency ω was proportional to $E_o E_1$ or $H_o H_1$.[18,22] Another way is to measure the magnetic field dependence of the electric field susceptibility (for β)[19] or the electric field dependence of the magnetic susceptibility (for γ). Since the term βHEE (γEHH) is quadratic in the electric (magnetic) field, $2\beta H$ ($2\gamma E$) corresponds to the electric (magnetic) susceptibility.

In Fe_3O_4, the third order effect, $\partial EEHH$, was detected by measuring the magnetic field dependence of the electric susceptibility(ε), ε was dependent on the direction of the magnetization, but the reversal of the magnetic field, thus the magnetization, resulted in little difference of ε indicating that the effect is not due to the βHEE term but due to the $\partial EEHH$ term. (See Chap. 3.)

It should be noted here that the sign of the ME effect linear in E or H is dependent on the direction of the electric or magnetic polarization. The direction of polarizations should be determined before the experiment. If there are equal amount of domains with opposite direction of polarization, ME effect is not detectable. In the case of Cr_2O_3 where IR is a symmetry element and there is

no electric or magnetic polarization, the situation is a little different. In this case, an antiferromagnetic sublattice composes of one atomic site which shifts up or down along the c axis from the center of surrounding anions. (See Sec. 1-3.) The sign of the ME effect depends on the correspondence of these two kinds of sublattices and ME cooling, i.e., the simultaneous application of electric and magnetic field as the material is cooled through its Néel temperature T_N,[29,30] is necessary and effective to make a single domain crystal. In the course of ME cooling, one domain will have a lower energy than the other according to the direction of the electric and magnetic fields. In the case of Fe_3O_4, a ferroelectric ferromagnet, both electric and magnetic polarizations exist. If the directions of two polarizations are not determined, detected ME signal can not be reproducible.[10] The interrelation of two polarizations should be considered to make a crystal of single domain.

§ 1-3. Mechanisms of ME effect, in special reference to Cr_2O_3.

The first proposal of an atomic mechanism of ME effect was made by Rado[31] for Cr_2O_3. Cr_2O_3 crystallizes in the corundum structure. In this crystal, the point symmetry of a cation site is C_3 and the crystalline field has odd part along the c axis. There are two kinds of cation sites which are interchanged by an inversion. Each cation site composes antiferromagnetic sublattice and IR, not I, becomes a symmetry operation in the antiferromagnetic state. By the application of an external electric field along the c axis, cations in one sublattice is shifted to enhance the crystalline

field but it is reduced in the other sublattice and two sublattices become inequivalent. Rado pointed out that by such a shift of cations one-ion anisotropy constant D in one and the other sublattices increases and decreases, respectively, proportional to the applied field and resulted in the difference in the magnitude of two sublattice magnetizations. When the electric field is applied perpendicular to the c axis, axes of the crystalline field are tilted because of the odd part along the c axis. The tilting is in opposite sense for each antiferromagnetic sublattice. Thus, the easy axis of the spins is tilted from the c axis, in opposite sense for each sublattice, and total magnetic moment appears along the applied field. On the contrary to Cr_2O_3, α Fe_2O_3 has equal number of two kinds of cation sites in one antiferromagnetic sublattice. The effect of electric field is canceled out.

Rado[32] has calculated the effect of changes in the anisotropy constant on the molecular field approximation and explained the temperature dependence of α_{11} and α_{33} qualitatively except for the nonvanishing of α_{33} at low temperatures.

Quantitatively, however, so large electric field dependence of D is not expected as is necessary for Rado's theory to account for observed α. This was suggested by Date et al.[33] as they could not observe electric field shift of EPR line of Cr^{3+} in ruby. Instead of D, Date et al. proposed the electric field dependence of the intrasublattice exchange interaction (J) as the origin of the parallel effect at finite temperatures. However, this mechanism does not give any contribution to the perpendicular effect and can

not interprete the nonvanishing of α_{33} at 0 Kelvin. To explain the latter point, Alexander and Shtrikman[34] proposed another mechanism, electric field dependence of the g factor.

As for the perpendicular case, another mechanism was postulated by Hornreich and Shtrikman.[35] As the symmetry of Cr_2O_3 is lowered by the application of the electric field perpendicular to the c axis, antisymmetric exchange interaction can appear and spin canting results the total magnetic moment along the electric field.

Of these mechanisms, Hornreich and Shtrikman claimed for the parallel case of Cr_2O_3 that the electric field induced g shift is dominant at low temperatures and electric field dependence of the intrasublattice exchange is dominant at high temperatures and that of the one-ion anisotropy constant is dominant for perpendicular case. They calculated α and χ, the magnetic susceptibility, on the molecular field approximation. In the expression of α, the part equivalent to χ was substituted by the experimental results[36] and the temperature dependence of α was obtained. Above conclusion based on the comparison of the shape of this temperature dependence with the experiment.

Their argument was inevitably qualitative, and quantitative evaluation of each mechanism is impossible. If the electric field dependences of these parameters are temperature dependent, nothing can be concluded from the temperature dependence of α. Comparison with the data on ruby can not be definitive, too. Parameters can be different about one order of magnitude for Cr_2O_3 and $Al_2O_3:Cr^{3+}$. An example is the anisotropy constant D.[37]

To go one step further, some new experiments are necessary which make possible the separation of the contributions of each mechanism at any temperature.

§ 1-4. Possible applications of ME effect.

As mentioned § 1-1, ME susceptibility is closely connected to the magnetic symmetry of the crystal, which is determined by the spin structure. So, ME effect can be used

(i) to decide the magnetic crystal class of materials. Form of ME susceptibility tensor restricts possible magnetic crystal classes (see Table 1-I). The case of $GdAlO_3$[38] was an example.

In some cases, appearance of an element of the ME susceptibility tensor is the easiest way to detect the change of magnetic symmetry and thus ME effect can be used

(ii) to determine the magnetic transition point. The Neel point of $GeMnO_3$[39] and the pressure dependence of T_N of Cr_2O_3[40] were determined by ME effect. Spin flipping was observed through ME effect in $DyPO_4$[41] and Cr_2O_3.[23]

Near these transition points, ME effect can provide

(iii) a new critical exponent of the spin system. It has been found that the temperature dependence of α just below T_N is the same as that of the sublattice magnetization.[42,43]

(iv) If contributions of each mechanism are determined, ME effect provides new information on the electronic structure of transition metal ions, though interpretation of parameters might be rather difficult. One interesting possibility

that was suggested for Cr_2O_3 is the investigation of the structure of the impurity state by the ME effect. An anomalous temperature dependence was discovered in one crystal of Cr_2O_3 below 4.2 K. (See Sec. 2-2.)

(v) Applications of the ME effect as devices[8] such as gyrator, magnetic sensor, read only memory, etc., have been proposed but not realized yet, because of small ME susceptibility and the low T_N of ME materials discovered so far.

1-5. Construction of this paper.

The purpose of the present investigation is to study the ME effect of two magnetic oxides. Studies on the ME effect of Cr_2O_3 is described in Chap. 2 and that of Fe_3O_4 is presented in Chap. 3.

ME effect have been most extensively investigated so far in Cr_2O_3, experimentally and theoretically. However, since experimental results so far obtained were only the temperature dependence of α, contributions of machanisms have not been evaluated experimentally. Moreover, there are some doubt on the reported absolute value of α. In Chap. 2, precise static measurement of α by the use of SQUID magnetometer is reported in Sec. 2-2. Sec. 2-3 gives description of the electric shift of the antiferromagnetic resonance and proposes an experimental method to separate contributions of respective mechanisms. Though the experiment has been carried out so far only at 24 GHz, electric field dependence of g and D was determined at 4.2 K.

Studies on the ME effect of Fe_3O_4 are presented in Chap. 3. It is well known that first order transition occurs in Fe_3O_4 at

124 K. Charges of Fe ions in B site of spinel structure order at this temperature. Important role of phonons was pointed out recently. However, the situation is complicated and even the magnetic symmetry of low temperature phase has not been determined. In Sec. 3-2, determination of the magnetic symmetry of Fe_3O_4 at 77 K from ME effect was described. Dependence of ME effect on the direction of the magnetization was measured and analysed in Sec. 3-3 and the electric field dependence of the magnetic anisotropy was determined.

References

1) For early works, see T.H.O'Dell: The Electrodynamics of Magnetoelectric Media (North-Holland Publishing Co., Amsterdam, 1970) Chap. 1.
2) L.D.Landau and E.M.Lifshitz: Electrodynamics of Continuous Media (Addison-Wesley Publishing Co., Inc., Reading, Massachusetts, 1960), p.119.
3) I.E.Dzyaloshinski: Zh. Eksp. & Teor. Fiz. 37 (1959) 881. English translation: Sov. Phys.-JETP 10 (1960) 628.
4) D.N.Astrov: Zh. Eksp. & Teor. Fiz. 40 (1961) 1035. English translation: Sov. Phys.-JETP 13 (1961) 729.
5) V.J.Folen, G.T.Rado and E.W.Stalder: Phys. Rev. Lett. 6 (1961) 607.
6) K.Kohn: Jiseitai Hand Book, ed. S.Chikazumi, K.Ohta, K.Adachi, N.Tsuya and Y.Ishikawa (Asakurashoten, Tokyo, 1975) p.989 [in Japanese].
7) R.R.Birss: Symmetry and Magnetism (North-Holland Publishing Co., Amsterdam, 1970)
8) R.M.Hornreich: IEEE Trans. Magn. 8 (1972) 584.
9) D.E.Cox: Int. J. Magn. 6 (1974) 67.
10) G.T.Rado and J.M.Ferrari: Phys. Rev. B12 (1975) 5166. G.T.Rado and J.M.Ferrari: Phys. Rev. B15 (1977) 290.
11) A.N.Christensen, S.Quèzel and M.Belakhovsky: Solid State Commun. 9 (1971) 925.
12) A.N.Christensen and S.Quèzel: Solid State Commun. 10 (1972) 765.
13) M.Mercier and B.Cursoux: Solid State Commun. 6 (1968) 207.
14) M.Mercier, P.Bauer and B.Fouilleux: Compt. Rend. B267 (1968) 1345.
15) See Sec. 2-2.
16) G.T.Rado: Phys. Rev. Lett. 23 (1969) 644.
17) H.Schmid: Int. J. Magn. 4 (1973) 337.
18) M.Mercier: Int. J. Magn. 6 (1974) 77.
19) M.J.Cardwell: Phil. Mag. 20 (1969) 1087.
20) G.R.Lee: Ph.D. Thesis, University of Sussex (1970).
21) G.R.Lee, M.Mercier and P.Bauer: C. R. Coll. Int. Terres Rares, Paris, Grenoble (1970) p.390.

22) S.L.Hou and N.Bloembergen: Phys. Rev. 138 (1965) A1218.
23) S.Foner and M.Hanabusa: J. Appl. Phys. 34 (1963) 1246.
24) K.Hoshikawa: private communication.
25) G.Kaji, A.Tasaki and N.Kawai: unpublished.
26) E.Kita, G.Kaji, A.Tasaki and K.Siratori: AIP Conf. Proc. 34 (1976) 204.
27) G.T.Rado and V.J.Folen: Phys. Rev. Lett. 7 (1961) 310.
28) T.H.O'Dell: IEEE Trans. Magn. 2 (1966) 449.
29) S.Shtrikman and J.C.Treves: Phys. Rev. 130 (1963) 986.
30) T.J.Martin: Phys. Lett. 17 (1965) 83.
31) G.T.Rado: Phys. Rev. Lett. 6 (1961) 609.
32) G.T.Rado: Phys. Rev. 128 (1962) 2546.
33) M.Date, J.Kanamori and M.Tachiki: J. Phys. Soc. Jpn. 16 (1961) 2589.
34) S.Alexander and S.Shtrikman: Solid State Commun. 4 (1966) 115.
35) R.M.Hornreich and S.Shtrikman: Phys. Rev. 161 (1967) 506.
36) E.B.Royce and N.Bloembergen: Phys. Rev. 131 (1964) 1912.
37) S.Foner: Phys. Rev. 130 (1963) 183.
38) M.Mercier and G.Vellcoud: J. de Phys. 32 (1971) C1-499.
39) L.M.Holmes and L.G.Van Uitert: Solid State Commun. 10 (1972) 853.
40) G.Gorodetsky, R.M.Hornriech and S.Shtrikman: Phys. Rev. Lett. 31 (1973) 938.
41) L.M.Holmes and L.G.Van Uitert: Phys. Rev. B5 (1972) 147.
42) G.T.Rado: Solid State Commun. 8 (1970) 1349.
43) E.Fischer, G.Gorodetsky and S.Shtrikman: J. de Phys. 32 (1971) C1-650.

CHAPTER 2 EXPERIMENTS ON THE MAGNETOELECTRIC EFFECT OF Cr_2O_3

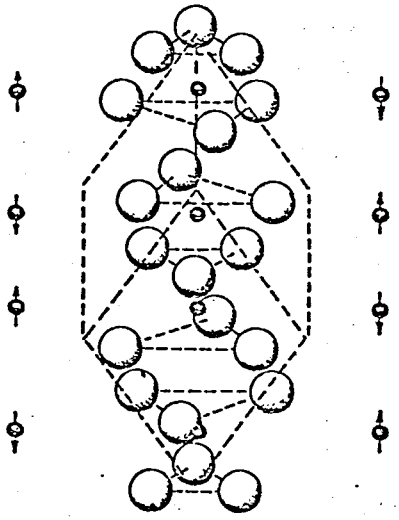

Corundum structure

§ 2-1 Introduction

Cr_2O_3 was the first ME material pointed out by Dzyaloshinski,[1] soon after the prediction of ME effect by Landau and Lifshitz.[2] Since then, many experimental and theoretical studies have been reported.[3-10]

The crystal structure is corundum type and the antiferromagnetic state is realized below T_N = 307 K. Spins are parallel to the c axis of the crystal and the magnetic symmetry is $\bar{3}'m'$ = $\{E, C_3, U_2, IR, S_6R, \sigma_dR\}$. In this case, only the bilinear effect is allowed and, if the biquadratic effect is neglected, the following relation holds.

$$\vec{M} = \tilde{\alpha}\,\vec{E}. \tag{2-1}$$

Here, $\vec{M}$ is the induced magnetization, $\vec{E}$ is the applied electric field and $\tilde{\alpha}$ is the magnetoelectric susceptibility tensor. For the discussion of the symmetry operation as shown in Sec. 1-1, C_3, U_2 and IR are necessary and sufficient in this case. Then, $\tilde{\alpha}$ of Cr_2O_3 is expressed as follows:

$$\tilde{\alpha} = \begin{pmatrix} \alpha_\perp & 0 & 0 \\ 0 & \alpha_\perp & 0 \\ 0 & 0 & \alpha_\parallel \end{pmatrix} \tag{2-2}$$

$\alpha_\parallel$ is the magnetoelectric susceptibility along the c axis corresponding to α_{33} in Table 1-I and $\alpha_\perp$ is that perpendicular to the

c axis corresponding to α_{11}.

To study atomic mechanisms of ME effect, the measurement of $\tilde{\alpha}$ should be performed carefully. Ordinarily, ac method with $1 \sim 100$ kHz was used to pick up small induced (magnetic or electric) polarization. However, spurious back ground signal due to the direct coupling of the input and the output circuits is proportional to the square of the frequency[7] and make it rather difficult, in practice, to determine the precise magnitude of $\tilde{\alpha}$. Determination of the sign of $\tilde{\alpha}$ is also not easy. In the static method, there is no problem in these points but very high sensitivity is required.

Recently, superconducting quantum interference device (SQUID),[11] which is a usefull application of Josephson effect,[12] was developed and applied to many ploblems in physics, earth science and biology.[13-15] This is a static high sensitive detector of the magnetic flux and provides a practical and sensible method of detecting magnetoelectric effect. Determination of the sign and the magnitude of the magnetic flux induced in Cr_2O_3 by the application of the electric field will easily be performed. The linearity of the effect can be checked at the same time. Absence of the external magnetic field makes the stable operation of SQUID system very easy.

To separate contributions of mechanisms of ME susceptibility, not only the precise value of ME susceptibility α but also a new experiment on ME effect are necessary as was described in Chap. 1. The measurement of the electric shift of the antiferromagnetic resonance (AFMR) in Cr_2O_3 is proposed and examined as the new experiment.

When the electric field is applied to Cr_2O_3 along the c axis, the g factor, the anisotropy constant D and the intrasublattice exchange J are changed a little, according to the proposed three mechanisms. (See Sec. 1-3.) The change of D, for example, affects α through the change of the thermal average of sublattice magnetizations. In addition to this, the change of D has a direct influence on the antiferromagnetic resonance point. Thus, observation of the electric shift of AFMR will supply another sort of information on the ME effect.

The studies of electric shift in the spin resonance were reported in the case of paramagnetic resonance (EPR). For example, Royce and Bloembergen[16] observed electric shift in EPR of Cr^{3+} in ruby which is a magnetic impurity in a diamagnetic material. In this case, the site symmetry of cations is C_3 and there is an odd part of the crystalline field parallel to the c axis. The site of Cr^{3+} is divided into two when the electric field is applied along the c axis. The EPR line was splitted into two, linearly to the strength of the applied electric field, but the center of it remained unchanged. Splitting of 70 Oe was observed at 170 kV/cm. This magnitude was much larger than the line width, $\simeq$ 20 Oe, and static measurement was possible.

In the case of AFMR of Cr_2O_3, the resonance line was much broader and static measurement was impossible. Change of the microwave power due to the electric shift of the resonance point was detected by ac method, as is the case of the usual magnetic field modulation. It is to be noted that AFMR does not split but shift

by the application of the external field.

In this chapter, we will report investigations on the ME effect of Cr_2O_3. The chapter is composed of two parts. In Sec. 2-2, the first part, the precise measurement of ME susceptibility of Cr_2O_3 by the use of SQUID magnetometer is mentioned. Experimental apparatus are described in Sec. 2-2-1 and results in Sec. 2-2-2. The technical points of the magnetometer and the comparison of our results with the previous data by ac method will be discussed in Sec. 2-2-3. An interesting and unusual temperature dependence of α discovered in one crystal will also be reported. In Sec. 2-3, the second part, the effect of electric field along the c axis on the AFMR of Cr_2O_3 is stated. Sec. 2-3-1 gives the formulation. Experimental details are described in Sec. 2-3-2. Sec. 2-3-3 gives the analysis of the experimental result. The electric field dependence of the anisotropy constant is deduced and discussed, compared with the case of Cr^{3+} in ruby.

§ 2-2 Precise Measurement of ME Susceptibility by the Use of SQUID Magnetometer

2-2-1 Experimental procedures

A SQUID magnetometer

A block diagram of the experimental arrangement is shown in Fig. 2-1. The present SQUID magnetometer was similar to SQUID magnetometer which were reported by other authors[15] except that there was no magnet to apply external field to the sample. The ordinary 2-holes type SQUID made of Nb was used. The holes were 2.5 mm in diameter. The weak contact was achieved by adjusting two NbTi screws, which could be turned by a worm gear from the outside of the cryostat. The SQUID was operated with rf bias of 22 MHz. For the field modulation, 1 kHz ac current was supplied to the rf coil which was placed in one hole of SQUID. The signal was detected phase sensitively by a lock-in amplifier and the output of the amplifier was fed back to the rf coil to operate the system as a null detector. Voltage of 26 mV induced by the feed back current across a standard resister R_f, 20 kΩ, corresponds to a flux quantum, ϕ_o. The output voltage was supplied to the y axis of a x - y recorder, whereas the dc voltage supplied to the sample was fed to the x axis. A dry battery and a 1 MΩ variable resister, potentiometrically connected, were used as a dc voltage supply up to 360 V.

The flux induced by the sample was picked up by an astatically wound superconducting coil, 5 or 10 turns in each direction, and

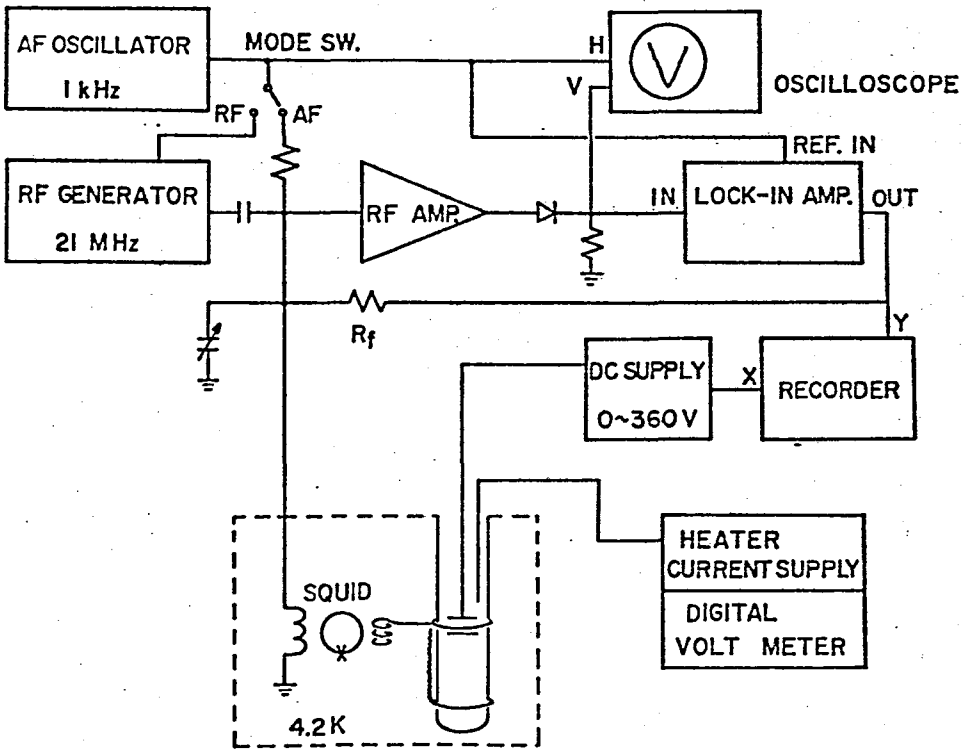

Eig. 2-1. Block diagram of a SQUID magnetometer for the measurement of magnetoelectric effect. The "staircase" pattern or the "triangle" pattern is observed in the oscilloscope according to the mode switch position, RF or AF.

was transferred into the signal coil placed in the other hole of SQUID. A signal coil was wound 80 turns on a quartz rod, 2.1 mm in outer diameter. NbTi wire of 0.075 mm diameter was used.

The sensitivity of the magnetometer as a whole was calibrated by a small coil with dimensions similar to the sample. A standard magnetization was induced by a known current through the coil and was detected. The sensitivity was 3.5×10^{-8} emu/mV or 1.0×10^{-7} emu/mV, depending on the pick up system.

To make the temperature of the sample below 4.2 K, the bath of liquid helium was pumped and the temperature was measured by the vapour pressure. To have the higher temperature of the specimen, keeping SQUID element at 4.2 K, another cryostat was constructed where the sample chamber was separated from the helium bath by a glass dewar of about 12 mm in inner diameter and 18 mm in outer diameter. In this case, the pick up coil became larger and sensitivity was lowered compared with the case without the inner dewar. A schematic illustration of this case is shown in Fig. 2-2. To make the temperature of the sample chamber homogeneous, a Cu pipe about 0.5 mm thick, 10 mm in inner diameter and 15 cm long was inserted as a heat sink and He gas of approximately 1 torr. was introduced. Manganin wire was wound non-inductively on the Cu heat sink as a heater. The temperature of the upper end of the heat sink was measured by AuCo-Cu thermocouple.

The vacuum space of the dewar was filled with He gas, at first, to cool the sample to 4.2 K and then evacuated. The temperature of the sample chamber was increased up to approximately 20 K by

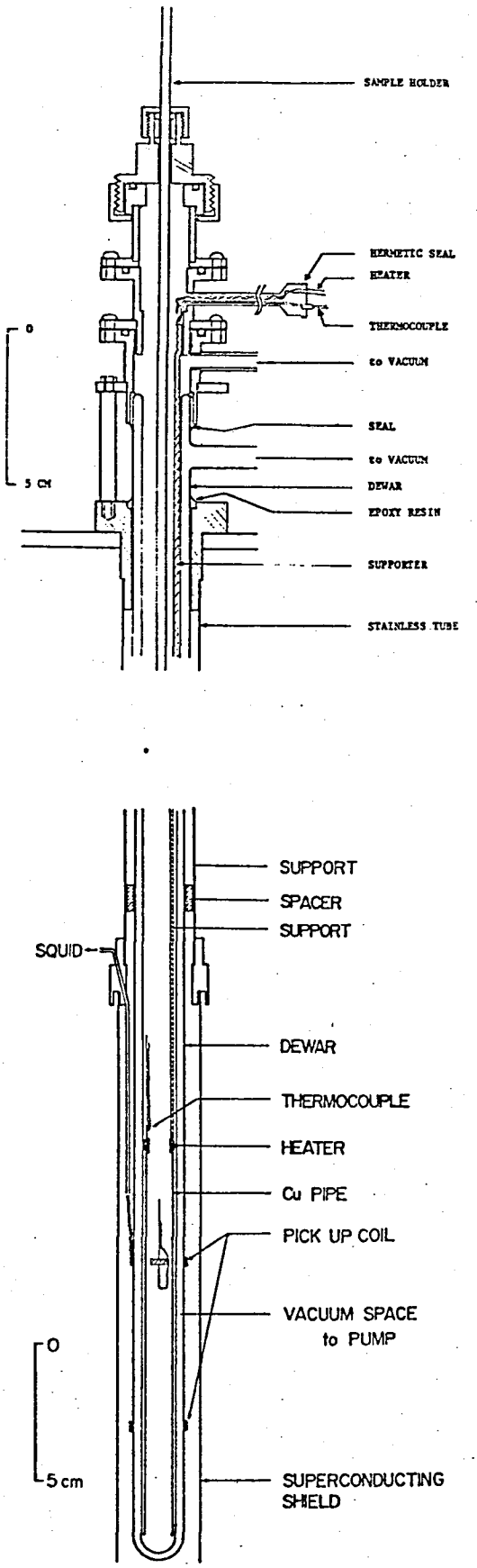

Fig. 2-2. The sample chamber of the high temperature cryostat.

the evacuation. To realize the sample temperature higher than this stably, current through the manganin heater was controled. Approximately 270 K, by ≃ 200 mA, was the highest temperature of our system, because of the poor heat insulation of the glass dewar.

The difference of the measured temperature from that of the specimen was checked by a AuCo-Cu differential thermojunction. Below 170 K, the difference was smaller than 1 K but it was larger than 5 K when the temperature was higher than 250 K. In the highest temperature region, the temperature difference depends on the process of the heating. By the correction of this temperature difference, the accuracy of the measurement of the temperature was estimated to be better than 0.5 K when the sample temperature was below 200 K but ≃ 2 K at 250 K.

2-2-2 Specimens

Two specimens were cut from one single crystal. Sample I was a platelet parallel to the c plane, 0.65 mm thick and 23 mg in weight. Another sample (sample II) was a rectangular parallelepiped, 2.0 × 2.2 × 2.85 mm in dimensions and 57 mg in weight. The faces were parallel to the c plane, σ_d plane and the plane perpendicular to both, respectively. No heat treatment was given after the cutting.

A sample cell was composed of a cylinder and two pistons of bakelite. To apply the external electric field to the sample, electrodes were made by painting silver paste on the opposite surfaces of the specimen. Copper foils were pressed to the electrodes mechanically by the bakelite pistons. Since Cr_2O_3 is neither piezoelectric nor piezomagnetic, pressure of pistons has no primary effect on the ME response of the specimen. The resistance of the

specimen was larger than 100 MΩ at room temperature in every case.

The sign and the magnitude of the magnetoelectric susceptibility, α, depend on the antiferromagnetic domain structure. To have a single domain crystal, ME cooling, mentioned in Sec. 1-2, should be applied to the specimen. Since $\alpha_{//}$ is approximately one order of magnitude larger than $\alpha_{\perp}$ just below T_N,[4] magnetoelectric cooling parallel to the c axis is more effective than that perpendicular to it. 360 V was supplied to the electrodes on the c plane (0.65 mm or 2.85 mm separated) in the magnetic field of 12 kOe along the c axis. These values were much larger than the threshold value reported.[17] When the directions of the electric and the magnetic field were antiparallel during the cooling, α of almost the same magnitude (± 2%) was observed with reversed sign, compared to the parallel ME cooling. From the above considerations and facts, it was concluded that the specimen of single domain was obtained.

2-2-3 Results

An example of the measurement is shown in Fig. 2-3. Apparently, induced magnetic moment was proportional to the applied voltage up to 250 V. This linearity of the magnetoelectric effect was confirmed at any temperature for this crystal. The magnetoelectric susceptibility, α (cgs/g), is given by

$$\alpha = cV/mE, \qquad (2\text{-}3)$$

where c is the sensitivity of the system, 3.5×10^{-8} emu/mV in this case, V is the output voltage, m is the mass of the sample

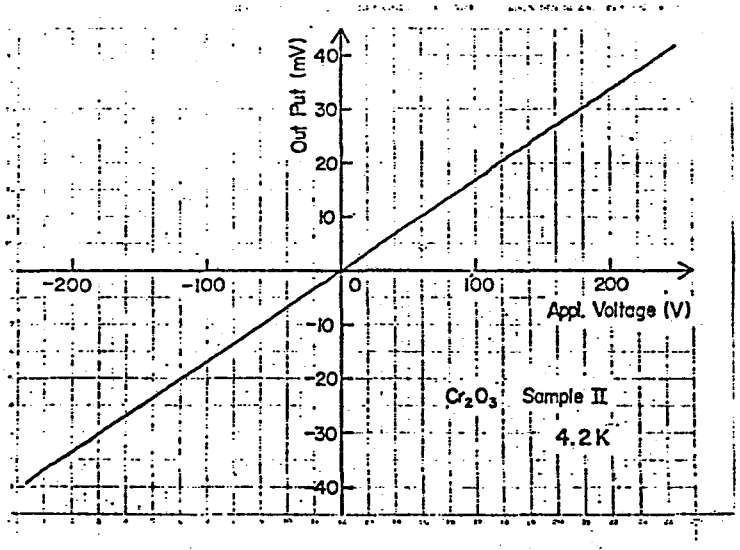

Fig. 2-3 A typical output of the magnetometer recorded against the applied voltage.

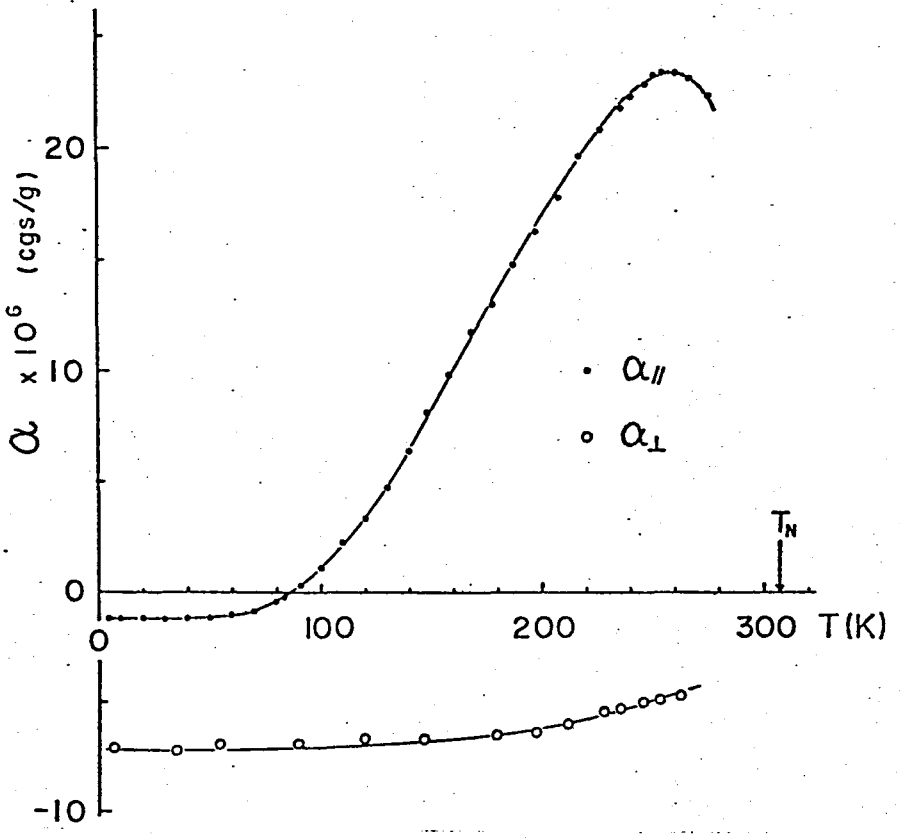

Fig. 2-4. Temperature dependence of $\alpha_{//}$ and $\alpha_{\perp}$ after parallel magnetoelectric cooling along the c axis. $\alpha_{//}$ crosses abscissa at 87 K.

and E is the applied electric field. The temperature dependence of α is shown in Fig. 2-4, for the parallel magnetoelectric cooling along the c axis. Qualitative feature of the figure is the same with the previous reports but the magnitude of the present result is larger than those except $\alpha_{//}$ at 4.2 K. (See Table 2-I.)

2-2-3. Discussion.

A. Noise.

The noise in the measurement of the magnetoelectric effect by the SQUID magnetometer consists of the noise from the device itself, from the temperature controle system and from the applied field.

The noise from the device was mainly due to the vibration of the superconducting magnetic shield relative to the pick up system in our case. This vibration causes local fluctuation of the magnetic flux. This noise detected at 4.2 K was about (1/100) ϕ_o. Pumping of the helium bath increased the vibration and resulted in higher noise level.

As for the temperature controle system, main problem came from heater current and the pulsive noise of a digital voltmeter to measure the electromotive force of the thermocouple. The latter can be avoided by the use of an analog device. The high frequency noise transported by conductors, the heater, the thermocouple and the lead wires to apply the electric field, to the pick up coil did not seem so large.

Though the heater was wound non-inductively, maximum current

of 200 mA shifted the triangle pattern of SQUID by about 2 ϕ_o. When the constant current supply was used and the current was not changed during the measurement, however, this shift was constant and did not cause the increase of the noise. If the heater and the thermocouple are placed far apart from the pick up coil, the noise of this origin can be decreased, but the controle and the measurement of the sample temperature will be less accurate.

In the case of the measurement of the magnetic susceptibility by SQUID, the device was directly influenced by the fluctuation of the applied magnetic field. If the measurement is carried out by the sweeping of the field, the precise compensation of the pick up coil is very difficult technically. If the sample is moved in the constant external field, the vibration accompanied by this movement causes additional noise. In the measurement of the magneto-electric effect, there is no such problems as the electric field does not couple with SQUID. However, the current associated with the supplied voltage can be the origin of the noise. In the present case, the resistivity of Cr_2O_3 is so high, especially at low temperatures, that we can neglect the current through the sample. Even if a current of 1 μA through a one turn coil of 5 mmϕ at the position of the specimen resulted in only (1/20) ϕ_o shift of the output. Since the current loop in the measurement is perpendicular to the pick up coil and the current was much smaller, the coupling of the current through the sample to the pick up coil should be much smaller. The effect of the charge up current of the capacitor, composed of the sample and the coaxial cable to it,

could be larger. This is proportional to the sweep rate and we changed 360 V by more than 5 s to suppress the effect. On the other hand, temperature dependence of the magnetic susceptibility of the material near the pick up coil led to a temperature dependent magnetization proportional to the trapped terrestrial magnetic field, and caused a drift of the output. When the measurement was carried out with changing temperature, sweep rate of the electric field should not be too low. Another noise source was again the digital device to measure the applied dc voltage or current. Analog devices should be used.

By the use of SQUID, the measurement of magnetoelectric effect can be carried out easily, by sweeping electric field. The sign and the magnitude of the induced moment can be directly determined against the applied electric field. The advantage over the usual ac method is that SQUID offers a mean of high sensitive static measurement.

B. Comparison of the present results with the previous reports.

In the present experiment, α was not obtained over the whole temperature range from 0 Kelvin to T_N. However, values characterizing the temperature dependence of α such as maximum of $\alpha_{//}$ ($\alpha_{//max}$), the temperature for $\alpha_{//max}$ (T_{max}), the temperature for $\alpha_{//} = 0$ ($T_{\alpha=0}$), $\alpha_{//}$ and $\alpha_{\perp}$ at 4.2 K ($\alpha_{//4.2K}$ and $\alpha_{\perp 4.2K}$) could be read in Fig. 2-4. Previous data by ac method and the present results are tabulated in Table 2-I. The present work gave largest values for α except $\alpha_{//}$ at 4.2 K.

The experimental error in $\alpha_{//}$ or $\alpha_{\perp}$ is brought about by the

Table 2-I Characteristics of the temperature dependence of α

Author	$\alpha_{//max}$ (cgs/g)	T_{max} (K)	$T_{\alpha=0}$ (K)	$\alpha_{//4.2K}$ (cgs/g)	$\alpha_{//max}/\alpha_{//4.2K}$	$\alpha_{\perp 4.2K}$ (cgs/g)
Astrov[3]	8.7×10^{-6}	255	80	0.6×10^{-6}	14.5	1.5×10^{-6}
Rado et al.[4]	3.	255	100			0.3
Mercier[5]	15.	270	120	2.0	7.5	
present work	23.	255	87	1.2	19.	7.

error in the calibration of the sensitivity, by the misorientation of the specimen and by the antiferromagnetic domain structure.

As for the orientation errors, the accuracy of the cutting of the crystal was estimated as $\lesssim \pm 1°$ and the misorientation between the c axis of the crystal and the axis of the pick up coil was estimated to be less than 3°. Error larger than 0.3 % can not be expected from this origin. Since $\alpha_\perp$ is 7.0×10^{-6} at 4.2 K, increase of 0.02×10^{-6} or 2 % is the upper limit to $\alpha_{//}$. Inversely at 255 K, increase of 0.07×10^{-6} or 1.5 % in $\alpha_\perp$ is the upper limit. The value of 87 K for $T_{\alpha=0}$ and the ratio $\alpha_{//max} / \alpha_{//4.2K} = 19$ support our conclusion that the setting errors were small.

The reproducibility of the value of α for both parallel and antiparallel magnetoelectric cooling strongly suggests that the specimen was single domain, the errors of the absolute values being within ± 2 %. The efficiency of the magnetoelectric cooling seems to be responsible for the large difference in the magnitude of $\alpha_\perp$ at 4.2 K between the present result and those in the previous reports. Errors on the calibration of the system are caused mainly by the difference of the geometry of the sample and the calibration coil. To check this point, the magnetic flux picked up by a coil was calculated.

Consider two coaxial coils with infinitesimal thickness on a plane. Total magnetic flux inside of the outer (pick up) coil is

$$\Phi = \int_0^t 2\pi r B_z \, dr = - \int_t^\infty 2\pi r B_z \, dr, \qquad (2\text{-}4)$$

where, t is the radius of the outer coil and the cylindrical coordinate is used. Integration in eq.(2-4) can be expressed as follows:

$$\Phi = \frac{4M}{t}\frac{1+a}{a^2}\left[\frac{1+a^2}{(1+a)^2}K(k^2) - E(k^2)\right]$$

$$= \frac{4M}{t}Y(a). \qquad (2\text{-}5)$$

Here, $a = d/t$, $k^2 = a/(1+a)^2$, K is the complete elliptic integral of the first kind and E is that of the second kind. M is the magnetization equivalent to the circular current through the inner coil:

$$M = \frac{IS}{c} = \frac{\pi d^2 I}{c}, \qquad (2\text{-}6)$$

where I is the current and S is the area and d is the radius of the inner coil, respectively. As is shown, Φ is proportional to M and the coefficient, Y, is dependent only on the relative size of coils, a. Y(a) was numerically calculated and plotted in Fig. 2-5. The difference of the area of the specimen ($\simeq$ 6 mm^2) and the calibration coil ($\simeq$ 11 mm^2) in the present case being considered, the error in the calibration was estimated $\simeq$ 7 % from Fig. 2-5.

These two origins of the error, antiferromagnetic domain structure and the calibration of the pick up system, always decrease the observed value. We suppose the present results have given more than 90 % of the true magnitude.

Since the characteristics of the magnetometer and antiferro-

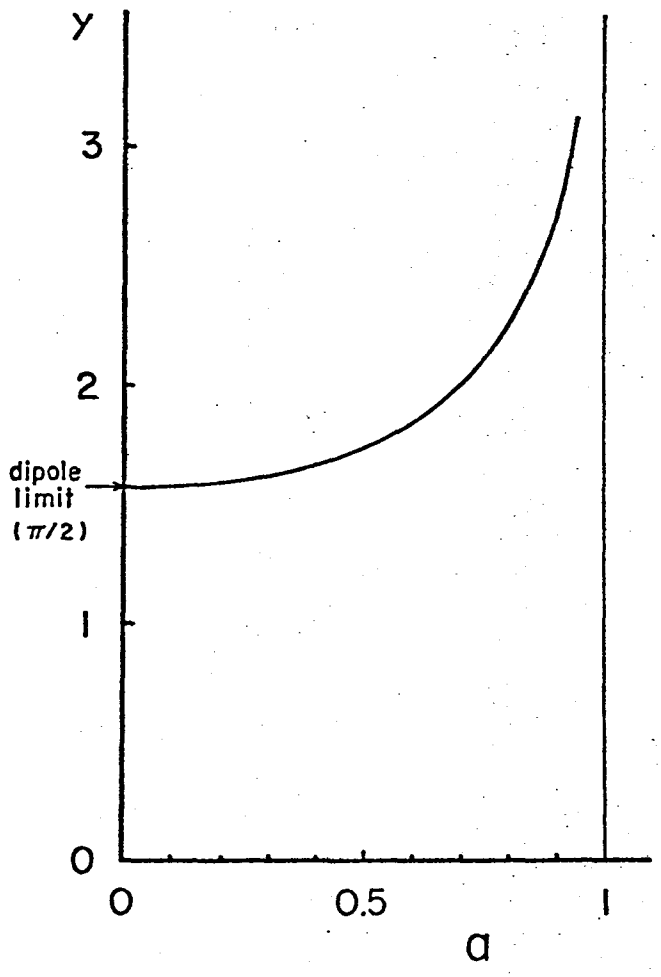

Eig. 2-5. Efficiency of the pick up as a function of the ratio a (= d / t).

magnetic domain structure were not affected by the temperature of the sample, only the setting error influences $\alpha_{//max}/\alpha_{//4.2K}$. The present value is much larger than those previously reported. Difference in the sample quality is supposed to be the main cause of the difference. In the case of Mercier, however, the reported value of $T_{\alpha=0}$ was too high and the tilting of the measuring direction from the c axis[18] seems to be responsible for the differences.

To interprete the present value for $\alpha_{\perp}$ at 4.2 K, 7×10^{-6} (cgs/g), by the tilting of the spin axis from the c axis, 3×10^{-3} radian/kV/cm should be assumed. Here, we used the values $\lambda = 8.5 \times 10^3$ and $K = 2 \times 10^5$ erg/cm^3, after Foner,[19] for the molecular field coefficient and the anisotropy energy, but, different from his suggested value, the sublattice magnetization was assumed to be 3 μ_B/Cr^{3+} = 583 emu/cm^3. This value of tilting should be compared with 1.6×10^{-5} radian/kV/cm, reported on Cr^{3+} ions in ruby.[16] This large difference between the values for Cr_2O_3 and Cr^{3+} in ruby is contrary to the parallel case, where the fractional change of D, the second order fine structure constant, was nearly the same for Cr_2O_3 and Cr^{3+} in ruby[20] (see Sec. 2-3).

The quality of the crystal is very important in the experiment on Cr_2O_3. It was reported that the introduction of small amount of Fe changed the magnetic structure.[21] The intensity of the antiferromagnetic resonance absorption was much influenced by mechanical or thermal treatment (see Sec. 2-3). In the measurement of the ME effect, we also found an extraordinary effect in one

crystal. Fig. 2-6 shows the temperature dependence, from 4.2 K to 1.6 K, of α for a crystal, origin of which is different from that mentioned above. α_A and α_B were measured along a direction 28° and 78° from the c axis, respectively. In both cases, parallel magnetoelectric cooling was adopted along the measuring axis. Fig. 2-7 shows the temperature dependence of α_A from 4.2 K to 250 K. In the low temperature region shown in Fig. 2-6, both $\alpha_{\parallel}$ and $\alpha_{\perp}$ should be constant, as was shown in Fig. 2-4, and the results shown in Fig. 2-6 are unusual. Anomaly in α_A is also exhibited in the high temperature region in Fig. 2-7. α_A crossed abscissa two times and higher order effect could be seen above 180 K. An example is shown in Fig. 2-8. At the same time, linear part at low external electric field decreased abruptly. (See Fig. 2-7.) Dashed line in Fig. 2-7 plots the linear part of the effect. The resistivity of this specimen was below 10 MΩ at room temperature and much lower than that of the specimen stated in Sec. 2-2-1 and 2-2-2. The apparent higher order effect, i.e., nonlinear response of the magnetization to the electric field, cannot be interpreted by the heat up due to the applied electric field, which could not exceed one degree. The temperature dependence of α shown in Fig. 2-7 also supports this argument. It is to be noted that existence of IR inhibits the β term in eq.(1-1) and the electric field dependence as shown in Fig. 2-8 cannot be expected in a perfect crystal of Cr_2O_3. No change in α was observed after an annealing at 1000°C for one day in the air. Though no impurity of more than 0.1 % was detected by chemical analysis,

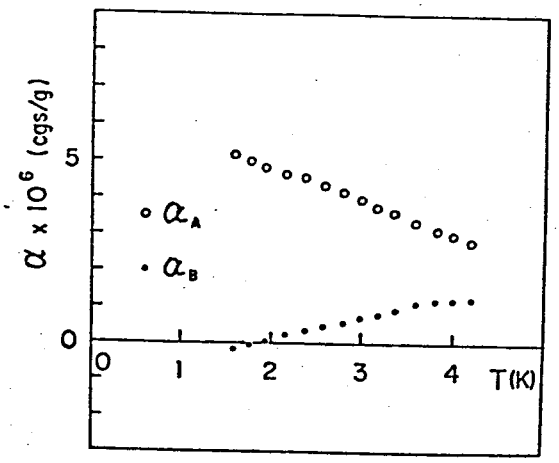

Fig. 2-6. Extraordinary temperature dependence of α below 4.2 K. Measuring direction was α_A: 28° α_B: 78° from the c axis, respectively.

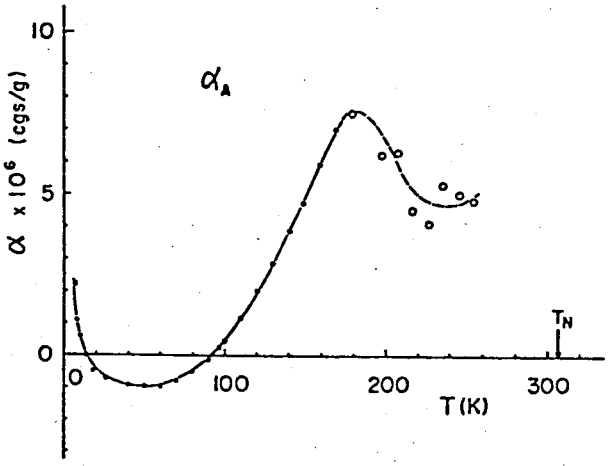

Fig. 2-7. Temperature dependence of α_A between 4.2 K and 250 K.

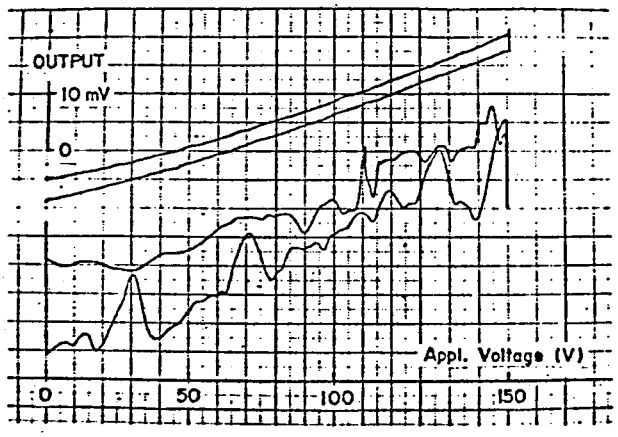

Fig. 2-8. Nonlinear dependence of the induced magnetic moment of the applied electric field at 250 K, for the crystal A. Two curves correspond to increasing and decreasing of the field. Lower part shows an example of unstable operation of SQUID when the He level was too low.

low lying excited states due to some impurities or lattice defects might be the cause of this anomaly. If this conjecture is true, ME effect can provide information on the impurity state of an antiferromagnet.

§ 2-3 Electric Shift in the Antiferromagnetic Resonance

2-3-1 Effect of the electric field on the antiferromagnetic resonance

At the beginning of this section, let us examine the effect of the electric field on the magnetic resonance of a ME antiferromagnet. The energy of an easy axis antiferromagnet consisting of 2N spins was written as follows:

$$\frac{\varepsilon}{N} = J_e \vec{S}_1 \cdot \vec{S}_2 - \mu_B \vec{H} \cdot [\, g_1 \vec{S}_1 + g_2 \vec{S}_2 \,] - [\, D_1 S_{1z}^2 + D_2 S_{2z}^2 \,]. \quad (2\text{-}7)$$

Here, suffix 1 or 2 denotes sublattices, S is the thermal average of spins, g is the g factor and D is the anisotropy constant. J_e is the intersublattice exchange constant and H is the external magnetic field. The intrasublattice exchanges were neglected since they do not affect antiferromagnetic resonance. We will confine ourselves to the case where both magnetic and electric field are parallel to the c axis. Directions of these fields and sublattice magnetizations are shown in Fig. 2-9. In the presence

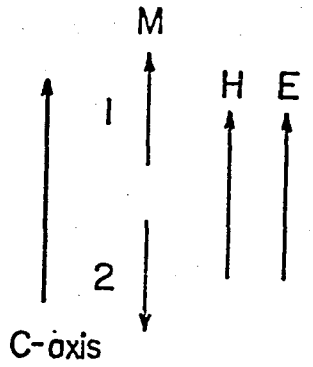

Fig. 2-9. The directions of the crystal c axis, magnetizations of two sublattices and externally applied electric and magnetic field.

of external fields, parameters on eq.(2-7) are expressed as

$$\begin{aligned} S_1 &= S_o + \delta S + \Delta S, \quad g_1 = g_o + \delta g, \quad D_1 = D_o + \delta D, \\ S_2 &= -S_o + \delta S + \Delta S, \quad g_2 = g_o - \delta g, \quad D_2 = D_o - \delta D, \end{aligned} \tag{2-9}$$

where δS, δg and δD are the electric field dependent part of each parameter and ΔS is that on the magnetic field. J_e is independent from the electric field since Cr_2O_3 has IR symmetry. δS, the change of the spin, is induced by the change of the intrasublattice exchange, δJ, and of the anisotropy, δD. In this sense, δD contributes twice in eq.(2-7).

The sign of δS, δg and δD is dependent on the antiferromagnetic domain structure. Parallel or antiparallel ME cooling reverses the sign of these. Parallel ME susceptibility is expressed as

$$\alpha_{//} = 2N \mu_B (g_o \delta S + \delta g S_o) / E. \tag{2-9}$$

The equation of motion of spins is

$$\hbar \frac{d \vec{S}_i}{dt} = g_i \mu_B \vec{S}_i \times \vec{H}_{eff\ i} . \tag{2-10}$$

$\vec{H}_{eff\ i}$ is the effective field acting on $\vec{S}_i$ and is written as

$$\begin{aligned} \vec{H}_{eff\ i} &= -\frac{\partial \varepsilon}{\partial \vec{M}_i} \\ &= \vec{H} - \frac{J_e \vec{S}_j}{g_i \mu_B} + \frac{D_i S_{iz} \hat{z}}{g_i \mu_B} . \end{aligned} \tag{2-11}$$

$\hat{z}$ is the unit vector along the z axis or the c axis. AFMR frequency

is given by solving the secular equation deduced from eqs.(2-7, 10,11). Substituting eq.(2-6), the result is expressed as

$$\hbar\omega = \sqrt{(J_e S_o + \delta g \mu_B H + 2D_o S_o + 2\delta D\delta S + 2\delta D\Delta S)^2 - J_e^2 S_o^2 + J_e^2 (\delta S + \Delta S)^2}$$

$$\pm [\, g_o \mu_B H + 2\delta D S_o + (2D_o - J_e)(\delta S + \Delta S)] \,. \qquad (2\text{-}12)$$

eq.(2-12) can be written as

$$\hbar\omega = \hbar\omega_o + \hbar\delta\omega$$

$$= \sqrt{4(J_e + D_o)D_o S_o^2 + J_e^2 \Delta S^2} \pm g_o \mu_B H + (J_e - 2D_o)\Delta S$$

$$\pm [(2D_o - J_e)\delta S + 2S_o \delta D] + \sqrt{4(J_e + D_o)D_o S_o^2}\ \frac{(J_e + 2D_o)\mu_B H}{4(J_e + D_o)D_o S_o}\,\delta g, \qquad (2\text{-}13)$$

where, the electric dependent part, δS, δg and δD, are taken into account up to the first order and the magnetic field dependent part, ΔS, is taken into account up to the second order. $\pm$ corresponds to branches of the resonance. $\hbar\omega_o$, the first three terms, gives the ordinary resonance frequency in the absence of the electric field. The last three terms, $\hbar\delta\omega$, indicate the shift produced by the electric field. According to Foner,[19] $J_e = 310\ cm^{-1}$, $D_o = 1.1 \times 10^{-2}\ cm^{-1}$ and $g_o = 1.97$ for Cr_2O_3 at 4.2 K. Then,

$$\hbar\delta\omega = \pm [\, 310\delta S - 3\delta D \,] + 3.8H\delta g \quad (cm^{-1}). \qquad (2\text{-}14)$$

Here, H is in the unit of kOe. If electric shift of the AFMR is measured at different frequencies, δS, δD and δg can be determined separately from eqs.(2-9) and (2-13).

2-3-2. Experimental.

AFMR in Cr_2O_3 was so broad that the electric shift could not be detected statically. This difficulty was avoided by the use of ac modulation method. The intensity of the signal observed by the electric field modulation was compared with that observed by the usual magnetic field modulation in the same experimental conditions before and after the electric field modulation measurement.

AFMR was observed using a standard reflection type microwave spectrometer (JEOL JES-ME-2X) of intra-faculty common utilization ESR room in our faculty. The frequency of the microwave was 24.2 GHz and a cylindrical cavity of TE_{011} mode was used. External magnetic field up to 60 kOe was generated by a superconducting magnet.

A block diagram of the experimental apparatus is shown in Fig. 2-10. The magnetic field was modulated by ac current at the frequency of 100 kHz through one turn coil in the microwave cavity. To check the phase of the signal carefully, lock-in amplifier (NF LI 573) was used instead of that built in the spectrometer, and the signal of the resonance was detected phase sensitively for 90° different phases of the reference signal. ac (100 kHz) high voltage supply was constructed by a power amplifier and transformer, connected to the magnetic field modulation current source. The reference signal to the lock-in amplifier was made by deviding the voltage of the ac current or voltage source. (See Fig. 2-10.) The strength of the magnetic field modulation

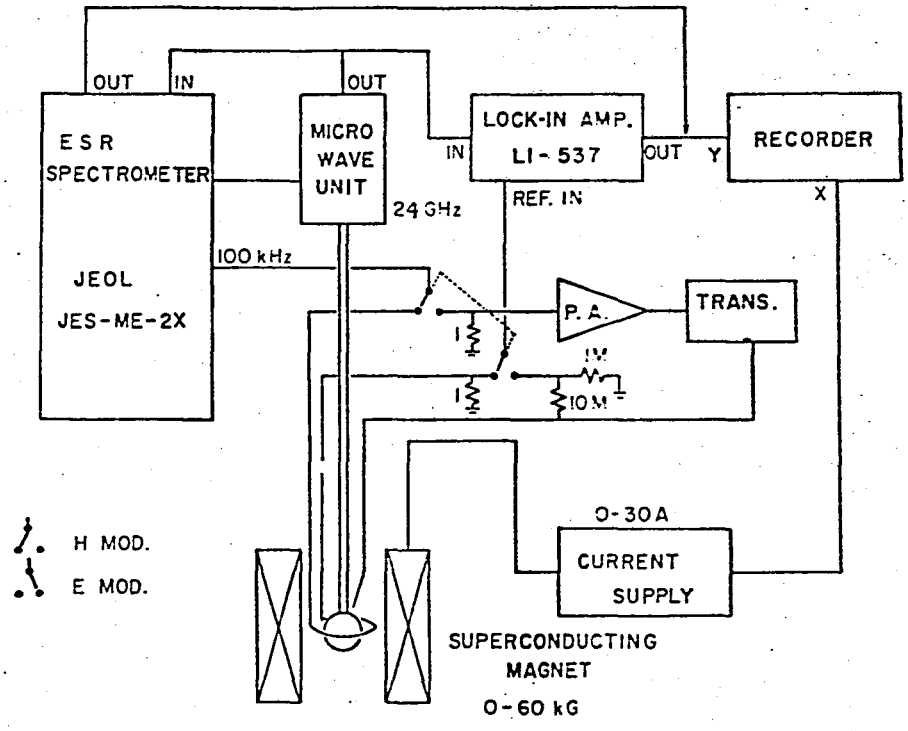

Fig. 2-10. Block diagram of a microwave spectrometer to measure the electric shift of AFMR. Magnetic and electric field modulation are selected by a switch.

used was up to about 1 Oe_{p-p} and that of the electric voltage modulation up to 360 V_{p-p}.

The single crystal used in the measurement of the parallel ME susceptibility in Sec. 2-2 was used in this measurement. However, the dimension of the specimen, 22 mg in weight, was so large that the Q value of the microwave cavity was lowered down and the measurement could not be performed. By grinding, the sample was formed in a platelet parallel to the c plane, 0.36 mm thick and 7 mg in weight. It is to be noted that the mechanical treatment such as grinding or cutting considerably weakened the signal of AFMR. The annealing at 1600° C for 1 day was necessary to recover the signal. Introduction and removal of the mechanical stress was supposed to give rise to the above changes.

To apply the ac electric field to the specimen, the electrodes should be attached. In an experiment of microwave frequency, the metal layer as an electrode must be thinner than the skin depth at the frequency. In the case of EPR, Royce and Bloembergen utilized the Ag film vapour deposited directly on the crystal.[16] In the present case, however, this method lowerd the Q value of the cavity remarkably and the experiment became impossible. Au and Cu-Al alloy (to decrease conductivity at 4.2 K) film deposited directly on the specimen appeared to be negative, too. This difficulty was avoided by using a Ag film of approximately 100 Å thick on a myler film as an electrode. Fine Cu wires were pressed to the electrodes by a thread as leads to the ac voltage supply. The sample and electrodes were set in a teflon holder as shown in

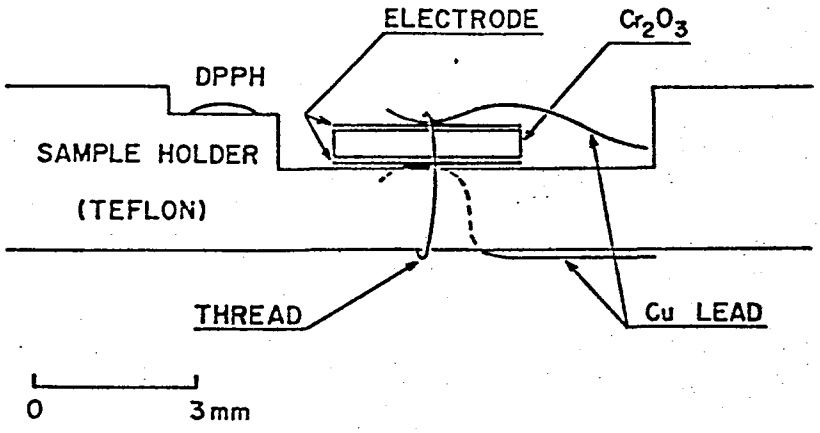

Fig. 2-11. Schematic illustration of the sample holder and electrode.

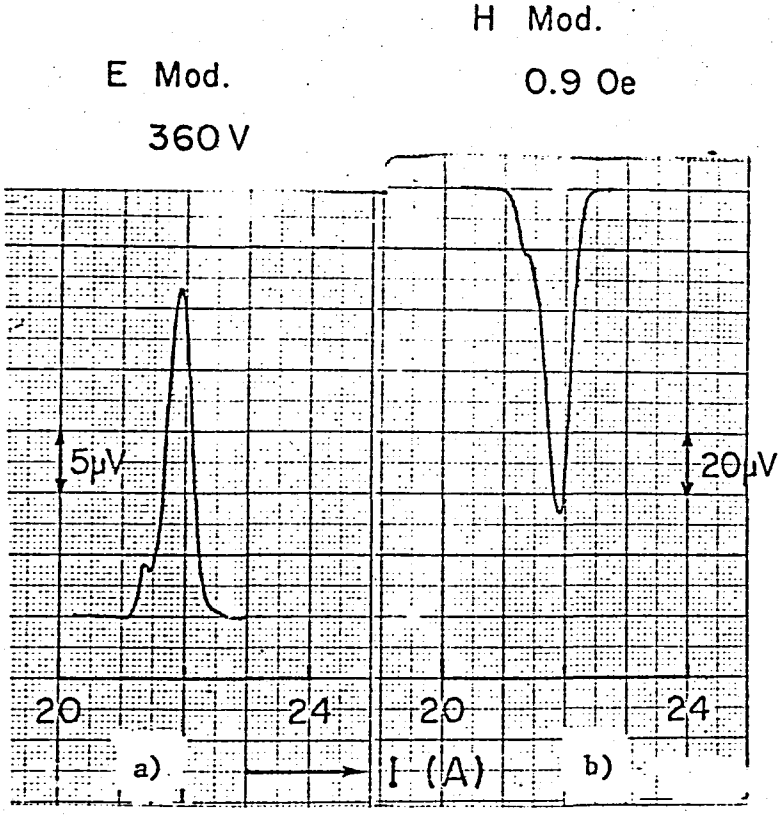

Fig. 2-12. The output of the resonance absorption vs. the current supplied to the superconducting magnet. 48 kOe was generated at 20 A.

a): electric field modulation with 360 V_{p-p}/0.4 mm.

b): magnetic field modulation with 0.9 Oe_{p-p}.

Fig. 2-11 and placed at the center of the cavity. Parallel ME cooling was adopted before the measurement.

An example of the signal was shown in Fig. 2-12. Usual differential curve of the absorption could not be obtained as the sample of 7 mg was too large for the spectrometer. AFC unit did not operate at the resonance point and the frequency of the microwave was not stabilized. By the magnetic field modulation, however, the signal was observed at the same position with the same line profile (Fig. 2-12b), just before and after the experiment by the electric field modulation. We could deduce the electric field shift of the AFMR by the comparison of these signals. The sign of the signal by the electric field modulation was inverted by the antiparallel ME cooling.

2-3-3. Discussion.

The amplitude of the signal with the 10 kV/cm of electric field modulation was equal to that with the 0.36 Oe magnetic field modulation. The change of the output due to the electric field modulation was the same, including its phase, as that of the magnetic field modulation with the external electric field applied parallel to the external magnetic field, the frequency of the AFMR is lowered when the parallel ME cooling is employed. Then the frequency shift was

$$\frac{\delta\hbar\omega}{E} = -3.4 \times 10^{-6} \ \text{cm}^{-1} / \text{kV/cm}. \qquad (2\text{-}15)$$

Since the experiment was carried out at 4.2 K, we can assume $\delta S = \Delta S = 0$* and $S_o = 3/2$. Then, $\alpha_{//} = -1.2 \times 10^{-6}$ cgs/g, observed in the same crystal[22] at 4.2 K gives

$$\delta g = -3.5 \times 10^{-8} \qquad \text{at } E = 1 \text{ kV/cm.} \qquad (2\text{-}16)$$

δD is deduced from eqs.(2-14), (2-15) and (2-16) as

$$\delta D = -1.1 \times 10^{-6} \ \text{cm}^{-1} \qquad \text{at } E = 1 \text{ kV/cm.} \qquad (2\text{-}17)$$

This is about one order of magnitude smaller than that reported for Cr^{3+} in ruby at room temperature.[16] This ratio is almost the same as the ratio of the fine structure constant (0.19 cm^{-1} for ruby[16] and 0.015 cm^{-1} for Cr_2O_3[19]**). It is interesting to note that if δD keeps its sign up to T_N, $\alpha_{//}$ due to the anisotropy mechanism is always negative and qualitatively conflicts with the observation.

---

* The validity of this assumption is not evident as χ of Cr_2O_3 is not 0 at 0 Kelvin.

** Contribution of magnetic dipole interaction was subtracted.

References

1) I.E.Dzyaloshinski: Zh. Eksp. & Teor. Fiz. 37 (1959) 881.
English translation: Sov. Phys.-JETP 10 (1960) 628.
2) L.D.Landau and E.M.Lifshitz: Electrodynamics of Continuous Media (Addison-Wesley Publishing Co., Inc., Reading, Massachusetts, 1960).
3) D.N.Astrov: Zh. Eksp. & Teor. Fiz. 40 (1961) 1035.
English translation: Sov. Phys.-JETP 13 (1961) 729.
4) D.J.Folen, G.T.Rado and E.W.Stalder: Phys. Rev. Lett. 6 (1961) 607.
5) M.Mercier: Rev. de Phys. Appl. 2 (1967) 109.
6) G.T.Rado: Phys. Rev. 128 (1962) 2546.
7) M.Date, J.Kanamori and M.Tachiki: J. Phys. Soc. Jpn. 16 (1961) 2589.
8) S.Alexander and S.Shtrikman: Solid State Commun. 4 (1966) 115.
9) R.Hornreich and S.Shtrikman: Phys. Rev. 161 (1967) 506.
10) K.Hoshikawa: private communication.
11) J.E.Zimmerman, P.Thiene and J.T.Harding: J. Appl. Phys. 41 (1970) 1572.
12) B.D.Josephson: Phys. Lett. 1 (1962) 251.
13) T.Fujita and T.Ohtsuka: Jpn. J. Appl. Phys. 15 (1976) 881.
E.P.Day: Phys. Rev. Lett. 29 (1972) 540.
14) J.S.Philo: Proc. Natl. Acad. Sci. USA 74 (1977) 2620.
M.Cerdonio, A.Congiu-Castellano, L.Calabrese, B.Pispisa and V.Vitale: Pro. Natl. Acad. Sci. USA 74 (1977) 4916.
15) E.J.Cukauskas, D.A.Vincent and B.S.Deaver Jr.: Rev. Sci. Instr. 45 (1974) 1.
M.Cerdonio and C.Messana: IEEE Trans. Magn. 11 (1975) 728.
16) E.B.Royce and N.Bloembergen: Phys. Rev. 131 (1964) 1912.
17) T.H.O'Dell: Int. J. Magn. 4 (1973) 239.
18) G.T.Rado and V.J.Folen: J. Appl. Phys. Supp. 33 (1962) 1126.
19) S.Foner: Phys. Rev. 130 (1963) 183.
20) E.Kita, K.Siratori and A.Tasaki: to be published in J. Phys. Soc. Jpn. 46 (1979) No. 3.
21) D.E.Cox, W.J.Takei and G.Shirane: J. Phys. Chem. Solid 24 (1963) 405.
22) E.Kita, A.Tasaki and K.Siratori: submitted to Jpn. J. Appl. Phys.

CHAPTER 3 EXPERIMENTS ON THE MAGNETOELECTRIC EFFECT IN THE LOW TEMPERATURE PHASE OF Fe_3O_4

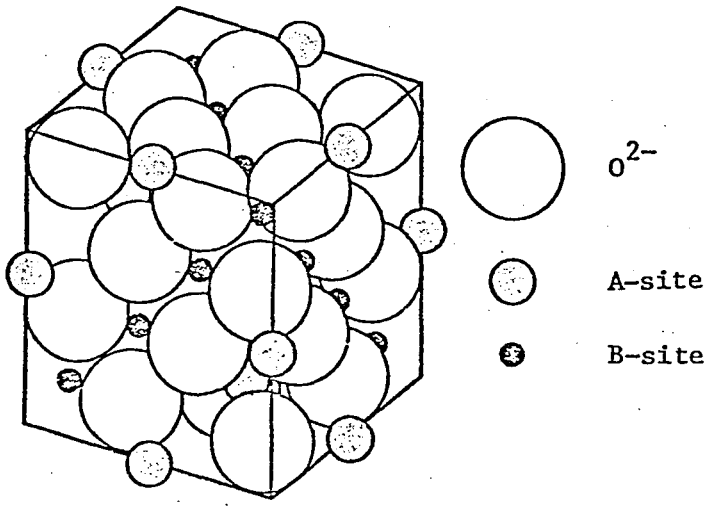

Fig. 3-1 Spinel structure

§ 3-1 Introduction

Magnetite, Fe_3O_4, is believed to be the oldest magnetic material known by Greek and used in their compass. More than two thousand years after, the magnetic properties was successfully analyzed by the theory of two sublattice ferrimagnetism developed by Néel. Fe_3O_4 has a spinel type crystal structure and the direction of spins of Fe^{3+} ions in the A site and that of Fe^{2+} and Fe^{3+} ions in the B site are opposite. The Curie point is about 860 K. Because there are equal numbers of Fe^{2+} and Fe^{3+} ions in the equivalent crystal sites, and they can interchange their positions by the exchange of one electron, instead of by atomic diffusion, electric conductivity as high as 10^2 ℧/cm is observed at room temperature. In 1928, anomaly was found near 120 K in the specific heat measurement[1] and suggested the existence of some sort of phase transition. It was found later that a discontinuous increase of electrical resistivity is accompanied by this transition.[2] It was natural to consider that the ordering of Fe^{2+} and Fe^{3+} ions in the B site is the origin of the transition.

In 1947, Verwey proposed a model of the charge ordering which is composed of alternate (001) layers of Fe^{2+} and Fe^{3+} ions.[3] (See Fig. 3-1.) In each layer, nearest neighbour sequence of B sites runs along [110] or [1$\bar{1}$0] direction, and hence the crystal has orthorhombic symmetry. In this paper, crystal indices refered to the cubic lattice will be used and [110], [1$\bar{1}$0] and [001]

axis, determined magnetically as will be shown below, will be called as a, b and c axis, respectively. The transition is often called as "Verwey transition".

Since then, magnetic, electrical and structural studies were carried out on the low temterature phase of magnetite. It was disclosed that the principal axes of magnetocrystalline anisotropy energy were the c (easy), the b (intermedeate) and the a (hard axis of the magnetization)[4] and supported the model of Verwey. In 1958, Hamilton[5] reported the observation of (002) neutron reflection and the Verwey model was considered to be proved and the problem to be settled.

In 1968, after one decade, the reflection spots with half integer indices were found in electron diffraction[6] by Yamada et al. and neutron diffraction[7] by Samuelsen et al.. After that, the low temperature phase transition of Fe_3O_4 has absorbed, once more, much interest of solid state physicists. The model of Verwey was finally rejected because (002) reflection observed by Hamilton was found to be a ghost due to the double reflection.[8] The important role of phonons, especially those having Δ_5 symmetry, was emphasized[9] and many studies on the magnetic and structural properties have been reported to elucidate the low temperature phase and the nature of the transition.

Among these, Rado and Ferrari reported the ME effect of this crystal at 4.2 K.[10] Since magnetite is a ferromagnet, macroscopically, this means that Fe_3O_4 is ferromagnetic and pyroelectric. Coexistence of the spontaneous magnetic and electric

moment was reported already on boracite family.[11] However, they are antiferromagnets and weak parasitic ferromagnetism appears in the ferroelectric phase. On the contrary, Fe_3O_4 is ferromagnetic in its basic properties. The feature of the coexistence of ferromagnetism and electric polarization in this case is interesting. In contrast to an antiferromagnet as Cr_2O_3, anisotropy of the ME effect could be directly observed by changing the magnetization direction, though the direction of the electric field was limited parallel to $[1\bar{1}0]$, $[11\bar{2}]$ or [111] axis in the present experiment. Phenomenologically, the change of magnetization of a ferromagnet due to the applied electric field is caused by a tilting and/or by a change in the magnitude of the magnetization. The former originates in the electric field dependence of the magnetocrystalline anisotropy, whereas the latter comes from the dependence of the exchange interaction and g factor as well as the magnetic anisotropy. Contributions of these two kinds of the mechanisms can be separated by measuring the magnetic field dependence of the effect.

On the other hand, the true symmetry of the crystal in the low temperature phase is still inconclusive. According to the recent structural studies, the low temperature phase of magnetite has a nearly rhombohedral lattice with an elongation along one of the cubic <111> axes,[8,12] whereas the magnetic principal axes are nearly along [001], $[1\bar{1}0]$ and [110].[13] Thus, the crystal symmetry of the low temperature phase should be $C_{2h} = \{E, C_2, I, \sigma\}$ or lower. If the elongation is along [111], the C_2 axis lies along $[1\bar{1}0]$ and σ is parallel to $(1\bar{1}0)$. The point is whether a $(1\bar{1}0)$

glide plane exists or not. Diffraction studies[12,14] suggested its existence, hence the crystal is monoclinic, but domain structure observation[15] and magnetoelectric effect measurement[10] gave negative results.

It might be necessary to note here the differences of our experiment from that of Rado and Ferrari.[10]

1° Difference of temperature

Their experiment was carried out at 4.2 K, whereas we measured the effect at 77 K. An anomaly at approximately 10 K was reported recently in the specific heat[16] and was attributed to a new phase transition. Then, there is a possibility that not only the magnitude but the symmetry of the magnetoelectric coefficient tensor are different at 4.2 K and at 77 K. As was stated in Chap. 1, this symmetry of the tensor reflects the symmetry of the crystal. It is to be noted that the diffraction studies[12,14] as well as the domain structure observation[15] were performed above 77 K.

2° Differece in the twin structure of the specimen

Rado and Ferrari implicitly assumed nearly orthorhombic symmetry and only the magnetic principal axes were fixed in their experiment. The axis of elongation was not determined uniquely. It seems also that they did not align the electric polarization of the crystal. So, coefficients of the ME effect could not be evaluated completely. On the determination of the symmetry, they argued that the symmetry of twinned crystals is higher than that of a completely detwinned crystal and their conclusion was correct even if their

specimen was twinned. Generally speaking, their argument is valid only if the volume of each twin domain is equal. If so, we cannot expect the ME effect to be observed. Accidentally in the present case, however, the glide plane in question is fixed uniquely by the fixing of the magnetic principal axes. In this sense, their conclusion is correct in principle.

3° Difference in the experimental method

Experiment of Rado and Ferrari was carried out in a static method or at the frequency of 1 kHz, mainly on the bc disk with electrodes on the a plane and the magnetization parallel to it. To discuss the symmetry of the crystal, they used an octagonal sample with the basis parallel to the ab plane and four pairs of lateral faces containing a and b planes. Electric polarization along the a and b axes induced by the magnetic field along the b axis were measured simultaneously. Our experiments were carried out at 10 $\sim$ 150 kHz, on a cube with (111), (11$\bar{2}$) and (1$\bar{1}$0) faces. Electric field was applied along one of these three axes and the changes of the magnetization along three axes were picked up. To determine the symmetry, we made much effort to eliminate spurious signals due to the misalignment of the crystal and that due to the non-uniformity of the electric field or the magnetization. We suppose that the same sort of problems also confront the static measurements of Rado and Ferrari but this point was not mentioned in their paper.

In this chapter, studies on the ME effect of Fe_3O_4 at 77 K are reported. Three subjects, 1) determination of the crystal

symmetry at 77 K, 2) electric field dependence of the magnetic anisotropy and 3) relaxation of the ME effect, were investigated.

Experimental procedures are given in Sec. 3-2. Preparation of specimens for the measurement is stated in Sec. 3-2-1. Measurement of the ME effect is described in Sec. 3-2-2. Sec. 3-2-3 gives the measuring method of electric susceptibility, which was carried out in connection with the relaxation effect.

In Sec. 3-3, experimental results were reported. Determination of the crystal symmetry is mentioned in Sec. 3-3-1. Dependence of the ME effect on the direction and the strength of the external magnetic field was measured and analyzed by spherical harmonics up to the fourth order in Sec. 3-3-2. Sec. 3-3-3 gives the relaxation of the ME effect. In connection with ME effect and its relaxation, magnetic field dependence of the electric susceptibility is described in Sec. 3-3-4.

Sec. 3-4 gives discussions on the present experiment. Dependence of the ME effect on the external magnetic field was interpreted in Sec. 3-4-1 by an assumption that a part of the magnetic anisotropy energy is closely connected to the electric polarization, whose magnitude and direction are affected by the electric field. Two possible directions of the electric polarization are proposed. The structure of Fe_3O_4 in the low temperature phase is discussed in Sec. 3-4-2, related to the charge ordering model recently proposed by M.Mizoguchi.

§ 3-2 Experimental Procedures

3-2-1 Crystal

Single crystals of Fe_3O_4 were synthesized at National Institute for Researches in Inorganic Materials by the floating zone melting method in an atmosphere of CO_2. They were subsequently annealed at about 1200°C for 20 hours within a $CO_2 + H_2$ atmosphere of a controlled oxygen partial pressure. This annealing was very important to have a good result. A cube of 4 mm edge, bounded by (111), $(11\bar{2})$ and $(1\bar{1}0)$ planes, was cut from the crystal and it was annealed for five days at 750°C in an evacuated and sealed off quartz tube. The transition temperature of the specimen, T_v, was 124 K. Au electrodes were vapour deposited on the opposite faces.

The crystal was imbedded in epoxi-resin within a frame of polymethyl metharylate (PMMA), (111) faces being kept exposed. The electrical contact with the electrode was achieved either by screws through the PMMA frame, in the case of $(11\bar{2})$ or $(1\bar{1}0)$ electrodes, or by lead wires directly soldered with In, in the case of (111) electrodes. Resistance of the specimen at 77 K was changed from approximately 3 to 8 kΩ, depending on the direction of the electric field.

The crystal was cooled to 77 K in an external magnetic field not less than 13 kOe, applied along [001] axis or along the direction 40° tilted from [001] to $[1\bar{1}0]$ axis. By this treatment, the axis of the crystal distortion, [111], and the magnetic

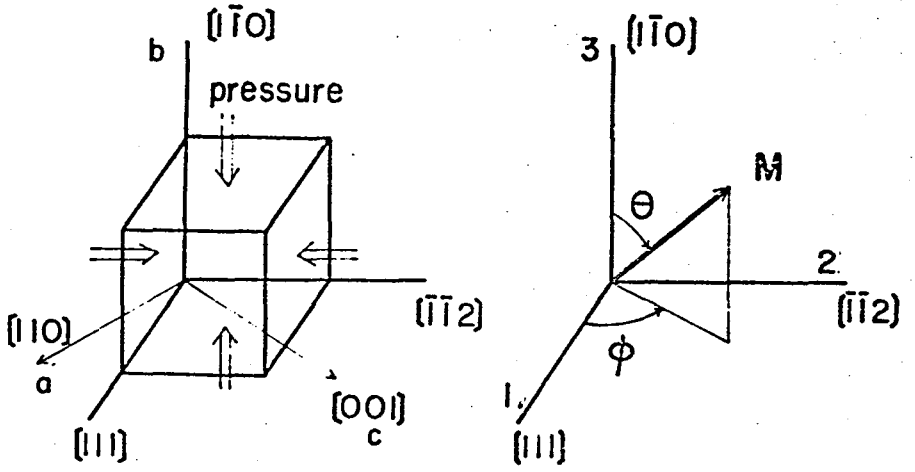

Fig. 3-2 Coordinate system and the setting of the crystal.

1, 2, 3: coodinate system used in this paper.

a, b, c: magnetic principal axes.

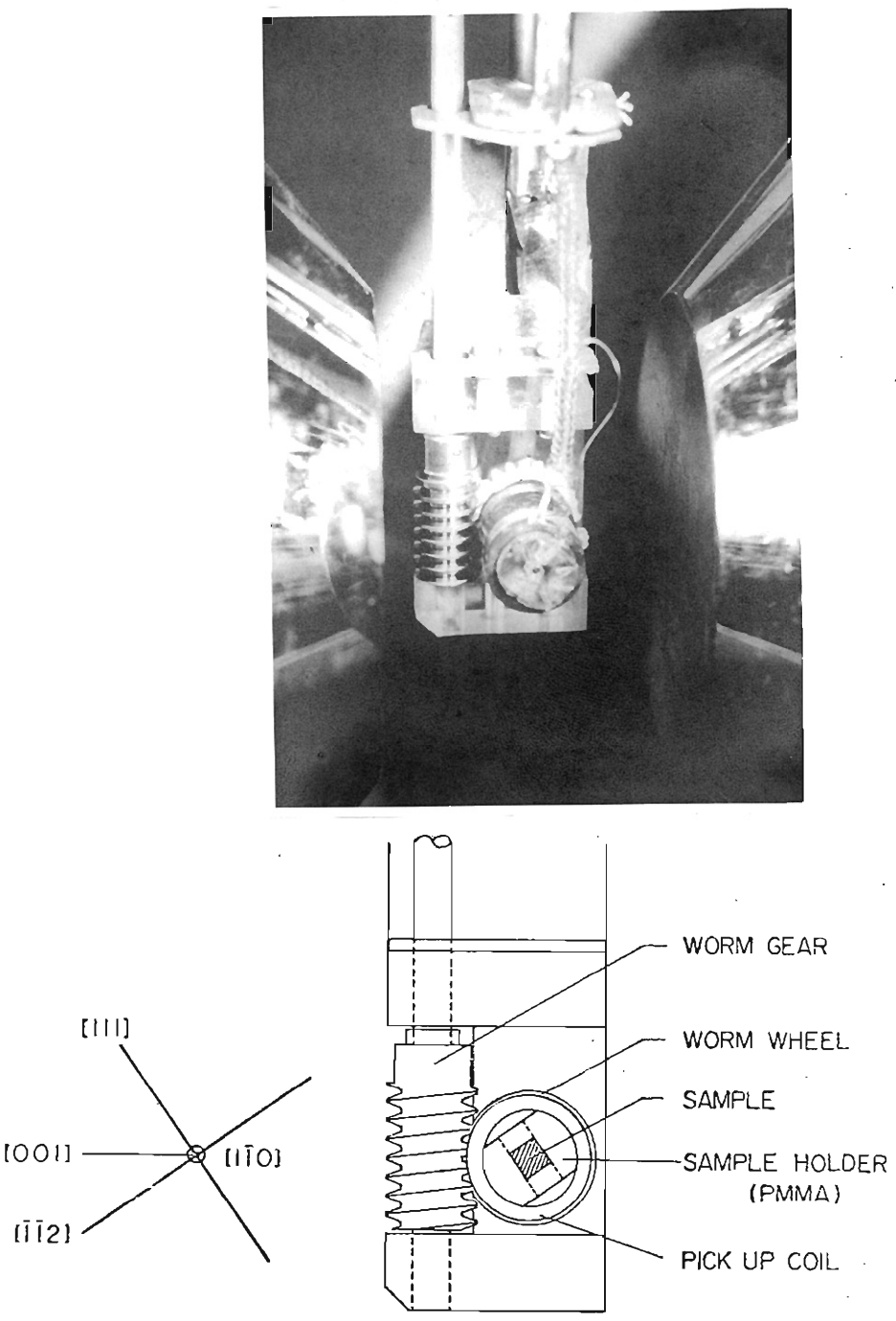

Fig. 3-3 A schematic illustration of the rotation mechanism of the specimen. The axis of the pick up coil is parallel to [1$\bar{1}$0] in the figure.

principal axes ([001]: the easy, [1$\bar{1}$0]: the intermediate and [110]: the hard direction of magnetization) were fixed. We will use the coordinate system shown in Fig. 3-2 and the polar coordinate, θ and ϕ measured from the axes [1$\bar{1}$0] and [111], to define the direction of magnetization or external field.

3-2-2 Apparatus

Oscillation of the magnetization due to the applied ac voltage was picked up by a coil whose axis was set along a cube edge, 1, 2 or 3 in Fig. 3-2, and it was detected phase sensitively. The frequency of the ac voltage was between 10 kHz and 150 kHz, mainly at 10 and 100 kHz. To calibrate the sensitivity of the pick up system, a three turn coil was set in place of the specimen and the output of the phase sensitive detector was measured at each frequency corresponding to a standard ac current through this coil. As the back ground level was not so low and we did not know the phase of the true signal, not only the magnitude but also the phase of the output was measured. Output with 90° different reference phases were plotted vectorially.

To determine the anisotropy of the magnetoelectric effect, the specimen was rotated around the horizontally set [1$\bar{1}$0] axis by a worm system, schematically shown in Fig. 3-3. Since a magnet was rotated around the vertical axis, the direction of the magnetic field could be changed stereographically. External magnetic field of 8.4, 10, 12 and 15 kOe or 8.4, 12, 17, 23.3 and 31.4 kOe were applied.

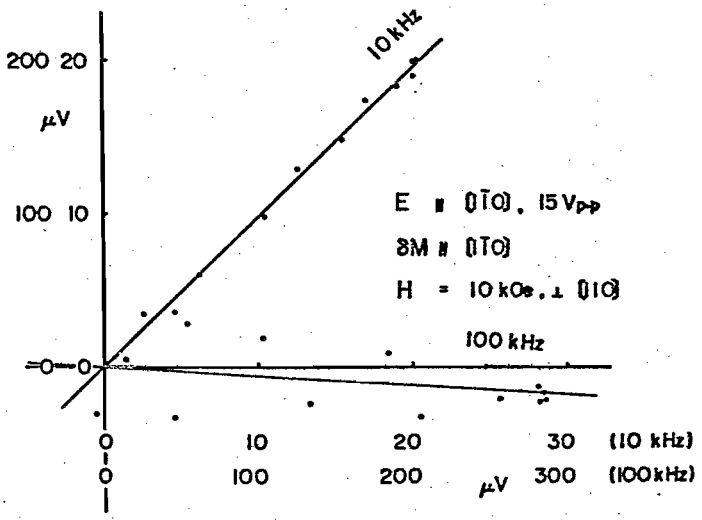

Fig. 3-4 Examples of the vector plot of the output.

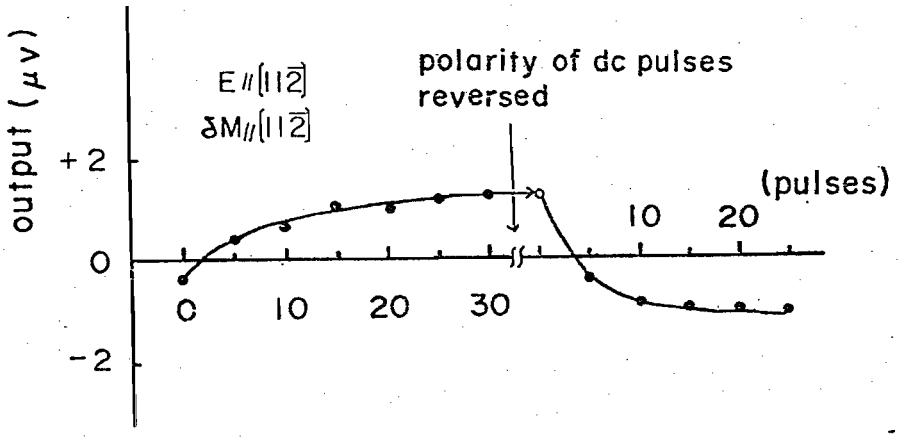

Fig. 3-5 Effect of dc pulses, 2 kV/cm × 0.7 msec, on the output.
magnetic field: 13 kOe along [001],
ac electric field: 13.5 kHz, 52 V_{p-p}/0.4 cm, along [11$\bar{2}$],
signal pick up: along [11$\bar{2}$].

3-2-3 Measurement of ME effect

A Temperature

All the experiments were carried out at 77 K.

B Phase and magnitude of output

To eliminate the back ground leakage due to the current through the sample and lead wire, measurements were repeated for the two opposite directions of the magnetization. The difference of the two outputs is plotted in Fig. 3-4. The coordinate and the abscissa of the figure correspond to two components of the output for 90° different reference phases. Direction of the magnetization within the (110) plane is an implicit parameter of the plot. As is shown, the points measured at 10 kHz lie on a straight line which crosses the origin and we can safely assume that this line gives the coordinate to the signal. When the measurement was carried out at 100 kHz, data points lie on a curve like an ellipse or hyperbola, whose axis crosses the origin. Apparently, there is some leakage output, which increases with increasing frequency. We assumed that the major axis of the curve was the coordinate of the signal in this case and neglected the transverse component. The difference of these two coordinates, for 10 kHz and for 100 kHz, is due to the relaxation of ME effect which will be discussed later.

C ME poling

Ordinarily, ME cooling is effective to achieve a single phase of a crystal that exhibits ME effect.[18] However, the electrical conductivity of Fe_3O_4 at T_v is so high that a sufficiently strong

electric field cannot be produced within the crystal. Instead of ME cooling, pulsed dc electric field of approximately 2.5 kV/cm and 0.7 msec duration was applied repeatedly at 77 K, with fixed magnetization direction (: ME poling). Higher voltage or longer duration was not possible in our case, because of the heating up of the specimen. Even the above mentioned pulses slightly affected the electrical contact. After one cycle of heating - cooling - poling, resistance of the specimen increased by approximately 10 Ω. In Fig. 3-5, oscillating magnetization along $[11\bar{2}]$ induced by the electric field in the same direction was picked up and plotted against the number of pulses along $[11\bar{2}]$. During the poling, the magnetization was kept along [001]. When the polarity of dc pulses was reversed, the signal changed its sign. Thirty pulses almost saturated the output in this case.

D Direction of magnetization

The equilibrium position of the magnetization was calculated from the external magnetic field by the following equations:

$$\partial\varepsilon^{o}/\partial\theta = 0, \qquad \partial\varepsilon^{o}/\partial\phi = 0, \tag{3-1}$$

$$\varepsilon^{o} = \varepsilon_{Z} + \varepsilon_{A}, \tag{3-2}$$

where ε_Z and ε_A are Zeeman and magnetic anisotropy energy given by

$$\varepsilon_{Z} = -\vec{M}\cdot\vec{H},$$

$$\varepsilon_{A} = K_{a}\alpha_{a}^{2} + K_{b}\alpha_{b}^{2} - K_{u}\alpha_{111}^{2} + K_{aa}\alpha_{a}^{4} + K_{ab}\alpha_{a}^{2}\alpha_{b}^{2} + K_{b}\alpha_{b}^{4}.$$

Here, α_i is the direction cosine of the magnetization to the axis i. (See Fig. 3-2.) According to Matsui et al.[17],

$$M = 505 \text{ G/cm}^3,$$

and Abe et al.[13] gave following values for K's, at 77 K:

$$K_a = 25 \times 10^5 \text{ erg/cm}^3, \quad K_b = 4.6 \times 10^5 \text{ erg/cm}^3,$$
$$K_u = 0.5 \times 10^5, \quad K_{aa} = 1.3 \times 10^5,$$
$$K_{ab} = 5.6 \times 10^5, \quad K_{bb} = 2 \times 10^5.$$

Here, K_{aa} and K_{ab} at 77 K were estimated on an assumption that the temperature dependence of them is the same as that of K_{bb}.

E Measurement

In a typical run of the experiment, ϕ_H, the azimuthal angle of the external magnetic field, was set at first by the rotation of the crystal. Then, the magnet was rotated to the calculated position to adjust θ, the polar angle of the magnetization, at a desired value. The azimuthal angle of the magnetization, ϕ, was calculated for each case. θ was changed within a limited range, from 45° to 135° when $\phi_H = 55°$ and from 70° to 110° when $\phi_H = 15°$, to avoid the switching of the magnetic principal axes. ϕ_H was changed from 15° to 95°. Thus, one run of the measurement, for a certain direction of the electric field and the pick up coil, was completed and the dependence of the magnetoelectric signal on ϕ for each θ and magnetic field strength were plotted.

F Absolute magnitude of signals

When one run of the measurement was finished, the specimen was warmed up to the room temperature and the plane of electrodes

or the pick up coil axis was changed. The next run of the measurement was started after the field cooling and the ME poling. The magnitude of the output for different runs could not be compared directly, since that depends on the total electric polarization of the specimen. The ME poling at 77 K was not so effective as the ME cooling in the case of Cr_2O_3 (see Sec. 2-2-3) and the relative magnitude of the ME tensor, normalized at the largest value, was scattered between 1 and 0.5. The value reported in Sec. 3-3 was the largest ones.

Even in one run of the measurement, depolarization or the decrease of the output appeared in some cases. Applied ac voltage was supposed to be the cause. To eliminate the effect of this depolarization, measurements for $\phi_H = 55°$ were repeated to monitor the electric polarization and the signals were normalized by the average of the monitoring outputs. The depolarization was more remarkable when the angle between the magnetization and the easy axis, [001], was larger and the magnetic field was stronger.

3-2-4 Measurement of electric susceptibility

In connection with the magnetoelectric effect, efforts to measure the electric susceptibility were made by three terminal method at 1, 10, 100 and 1000 kHz. A YHP 4270A automatic capacitance bridge was used. The edge of the sample cube was 6 mm in this case and the area of the main electrode was approximately 2 mm^2. The sample was treated in the same way as described above,

except the electrodes on $(1\bar{1}0)$ or $(11\bar{2})$ plane and the electrical contact to it. The main electrode was composed of In soldering and the guard electrode was made by silver paste. A double piston was pressed to the electrodes by a phosphor-bronze spring, through a hole of 4 mm diameter cut in the PMMA frame and resin. (See Fig. 3-17.) During the poling, the main and the guard electrodes were connected. ME poling was important to have reproducible results. At 77 K, the dielectric loss of Fe_3O_4, or its electrical conductivity, is so high that more accurate measurement was impossible.

§ 3-3 Experimental Results

3-3-1 Experiments on the crystal symmetry

Fig. 3-6 shows examples of the signal as a function of ϕ, the direction of the magnetization in $(1\bar{1}0)$ plane. (See Sec. 3-2-3,D) The noise level was of the order of several tenths of μV in this case.

The breaking of symmetry in the low temperature phase will be reflected on the coefficient tensor of the magnetoelectric effect. Existence of a symmetry element eliminates corresponding elements of the tensor. Table 3-I shows extinction rules for the terms linear in $\vec{E}$ and quadratic in $\vec{M}$ in the free energy expression. According to Rado and Ferrari,[10] these are the main terms in magnetite, though there exist other terms such as quartic in $\vec{M}$ or quadratic in $\vec{E}$. The present experiments also confirmed this argument.

Signals shown in Fig. 3-6 are due to the terms $E_2M_1M_1$, $E_2M_1M_2$ and $E_2M_2M_2$ (solid and open circles) and the terms $E_2M_1M_3$ and $E_2M_2M_3$ (triangles). (For the coordinate system, see Fig. 3-2.) Note that the total magnetic moment confined in the $(1\bar{1}0)$ plane does not violate possible symmetry operations, C_2R and σR, where R is the time inversion operator. The nonexistence of inversion and twofold rotation is evident by Fig. 3-6. To draw a conclusion on mirror symmetry from the small values shown by triangles in the figure, however, we should eliminate signals due to the possible errors in the setting of the specimen.

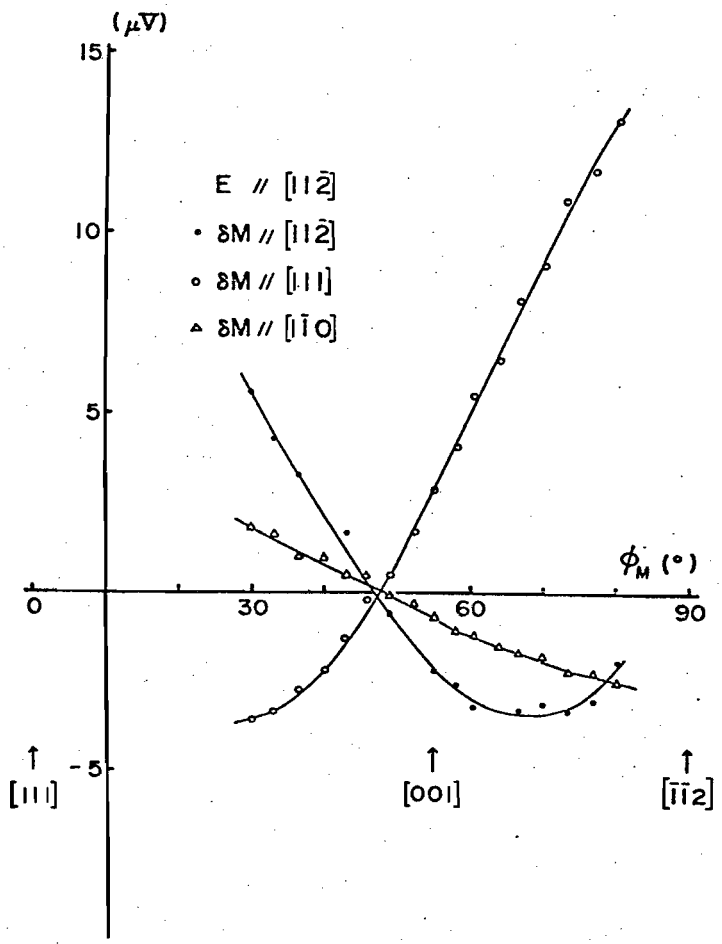

Fig. 3-6 Output after 40 - 70 pulses versus ϕ, the direction of the magnetization within $(1\bar{1}0)$. Experimental conditions are the same as in Fig. 3-5 except as indicated.

Indeed, the efficiency of the dc pulses along $[1\bar{1}0]$ suggests strongly that the crystal is nearly monoclinic. When the magnetization is confined in $(1\bar{1}0)$ plane, dc pulses showed little effect to increase the signal. If the magnetization was tilted to $[1\bar{1}0]$ axis by the application of the external field, dc pulses along $[1\bar{1}0]$ was very effective. The phase of the signal can be reversed by changing the direction of the magnetization tilting. This means that the electric polarization lies almost within $(1\bar{1}0)$ plane but rotates to $[1\bar{1}0]$ or $[\bar{1}10]$ by the tilting of the magnetization from $(1\bar{1}0)$ plane to $[1\bar{1}0]$ axis. It is to be noted that this fact indicates atomic displacement due to the change of the magnetization direction. Then, observation of the intensity change due to the tilting of the magnetization does not make possible the separation of the nuclear and the magnetic part of the neutron diffraction in the case of Fe_3O_4 below T_v. (cf. Fig. 7 of the reference[8].)

The accuracy of the orientations of the electric field, the pick up coil and the magnetic field was estimated as approximately one degree or less. A signal in the order of 1 μV, or up to 1/15 of the maximum signals for other orientations of the electric field etc., was possibly caused by this error. Nonparallel component of the electric field at the edges of the electrodes or that of the magnetization due to inhomogeneous demagnetizing field will amplify these spurious signals.

Let us assume that mirror symmetry does exist. Then, two kinds of crystallographic domains with opposite electric

Table 3-I Extinction rules for the free energy, linear in E and quadratic in M, in a crystal of C_{2h} or lower symmetry. Each one of the symmetry operations written in the matrix eliminates the corresponding term. For the coordinate system, see Fig. 3-2.

	M_1M_1	M_1M_2	M_1M_3	M_2M_2	M_2M_3	M_3M_3
E_1	I, C_2	I, C_2	I, σ	I, C_2	I, σ	I, C_2
E_2	I, C_2	I, C_2	I, σ	I, C_2	I, σ	I, C_2
E_3	I, σ	I, σ	I, C_2	I, σ	I, C_2	I, σ

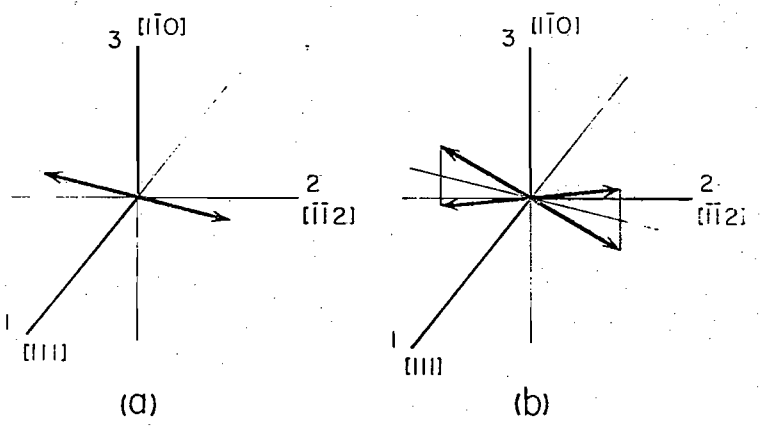

Fig. 3-7 Possible directions of electric polarization with (a) and without (b) the mirror symmetry. Directions of arrows in the b plane have no meaning. (See Sec. 3-4.)

polarization should exist in the squeezed and field cooled crystal. (See Fig. 3-7.) When an ac electric field is applied along $[1\bar{1}0]$ and the magnetization is rotated within (110) plane, perpendicular to the mirror plane, signals picked up along $[1\bar{1}0]$ should be symmetric with respect to [001] direction because of the mirror symmetry. Setting errors of the crystal, however, results in the signal which is antisymmetric with respect to [001]. This antisymmetric part must be proportional to the symmetric part, since both signals are proportional to the volume fraction of the two kinds of crystallographic domains, or the total electric polarization. The ratio of the antisymmetric part to the symmetric part depends only on the setting of the specimen.

On the contrary, if mirror symmetry does not exist, the electric polarization can deviate from $(1\bar{1}0)$ and there are four kinds of crystallographic domains in the specimen. (See Fig. 3-7.) In this case, there is an intrinsic antisymmetric part which is proportional to the $[1\bar{1}0]$ component of the total electric polarization, and this antisymmetric part need not be proportional to the symmetric part which depends on the $(1\bar{1}0)$ component of the total polarization.

Results of the experiment to clear up this point is shown in Fig. 3-8. All the signals are normalized to that at $\theta = 90°$. H- in the figure means that the measurements were carried out after the ME poling with $\theta = 50°$, less than 90°, whereas H+ indicates the ME poling with $\theta = 130°$. Signs after E indicate the polarity of the dc pulses. The setting of the specimen was

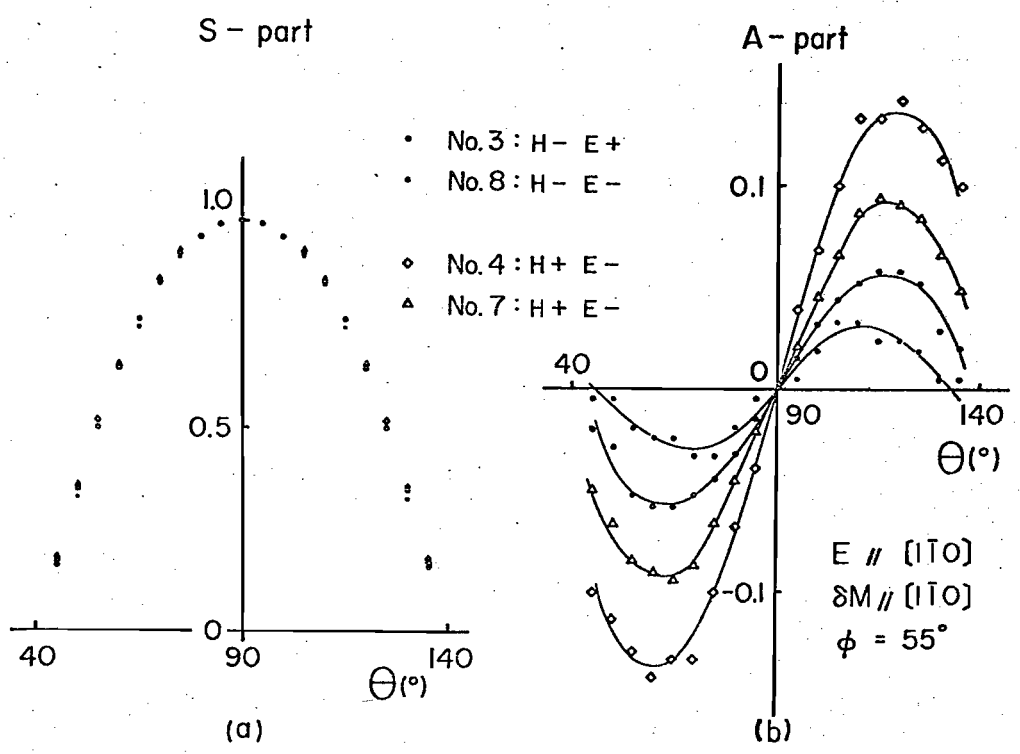

Fig. 3-8 Symmetric and antisymmetric part of the signal after the ME poling at $\theta = 50°$ (H–) and $\theta = 130°$ (H+). E+ or E– indicates the polarity of dc pulses. Signals are normalized at $\theta = 90°$. Experiment was carried out at 100 kHz, 15 V_{p-p}, along [1$\bar{1}$0].

kept unchanged throughout the measurement. Though the results are different up to several per cent from run to run, supposed to be due to the change in electrodes and/or lead wires, the difference between two groups, No.3, No.8 and No.4, No.7, in the antisymmetric part is evident. These four give the limit of the scattering of our results for each case. This proves that mirror symmetry does not exist and the magnetic symmetry of magnetite is triclinic at 77 K. As it is natural to assume that the symmetry of the low temperature phase is not higher than that of the high temperature phase, we can consider that the magnetic symmetry of magnetite at 4.2 K is also triclinic: the same conclusion as Rado and Ferrari.[10]

It is to be noted that the mirror plane in question is $(1\bar{1}0)$ in the rhombohedral domain with [111] or $[\bar{1}\bar{1}1]$ axis, but that is (110) in the $[1\bar{1}\bar{1}]$ or $[\bar{1}1\bar{1}]$ domain. Then, $[1\bar{1}0]$ pulses in the $[1\bar{1}\bar{1}]$ or $[\bar{1}1\bar{1}]$ domain with the magnetization in the (110) plane correspond to [110] pulses in the [111] or $[\bar{1}\bar{1}1]$ domain with the magnetization in $(1\bar{1}0)$ plane. Qualitative feature of [110] pulses is expected to be similar to $[11\bar{2}]$ pulses. (See Table 3-I.) If squeezing was not complete and the $[1\bar{1}\bar{1}]$ or $[\bar{1}1\bar{1}]$ domain existed in the specimen, symmetric part of the signal will appear, sign of which can be inverted only by the inversion of the polarity of dc pulses but not by the magnetic field direction during the poling. Difference of the results for the runs No.3 and 4 or 7 in the symmetric part indicates that the fraction of the $[1\bar{1}\bar{1}]$ and $[\bar{1}1\bar{1}]$ domain is less than several per cent. This limit is

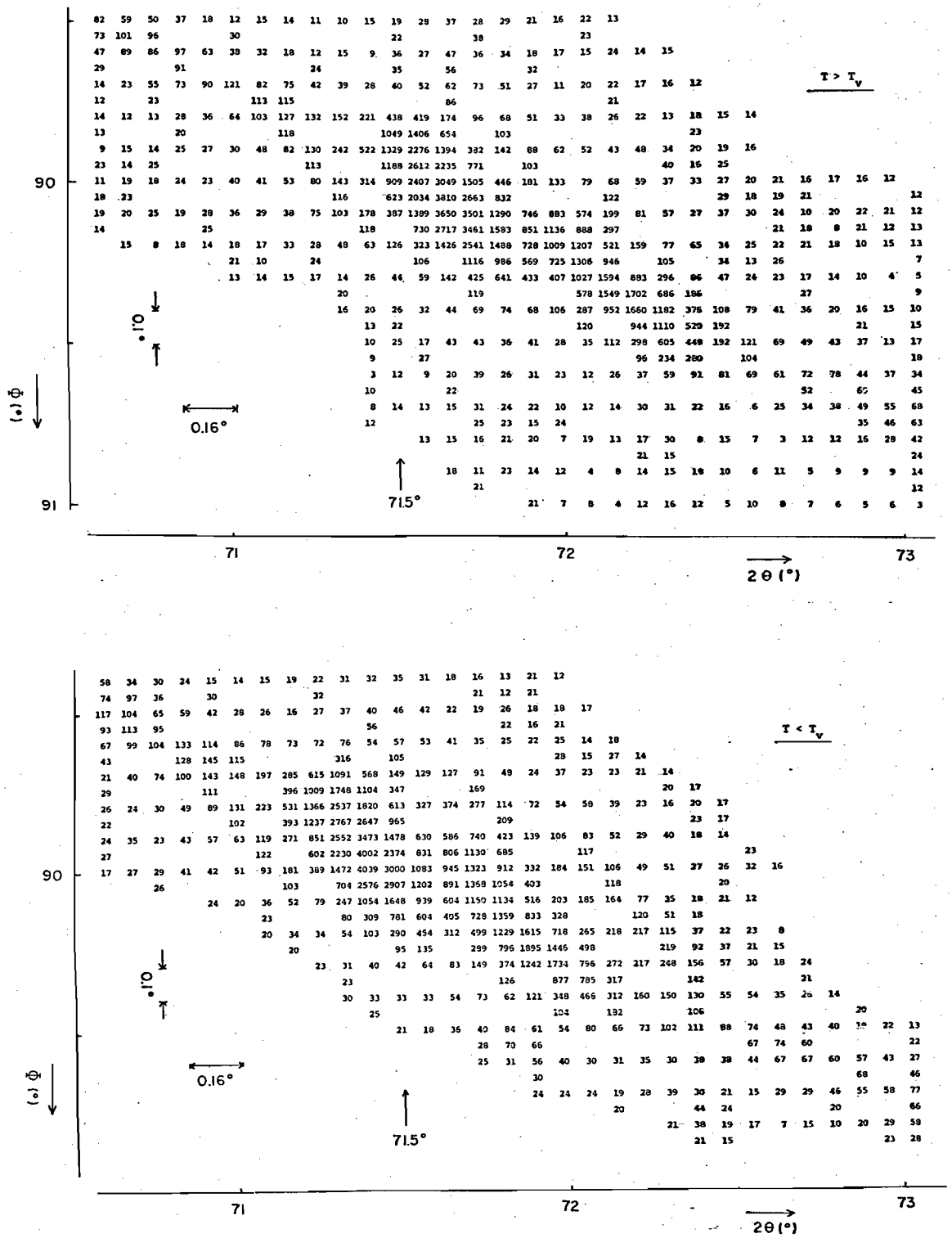

Fig. 3-9 The X-ray reflection intensity distribution in the two-dimensional reciprocal lattice space near (10,10,10) Bragg spot.

consistent with X-ray measurement.

By the rhombohedral distortion, a hhh Bragg spot splits into four, two of which lie within the $(1\bar{1}0)$ plane. According to the X-ray diffraction of our crystal with Mo Kα radiation, there is only one (10,10,10) reflection within the $(1\bar{1}0)$ plane below T_v, with larger lattice spacing than that above T_v. (See Fig. 3-9.) We expect that the fraction of domains, with the distortion axis other than [111], is smaller than several per cent.

3-3-2 Anisotropy of ME effect

As was reported in Sec. 3-3-1 in detail, Fe_3O_4 is nearly monoclinic at 77 K and signals were nearly symmetric or anti-symmetric to $(1\bar{1}0)$ plane. In other words, signals, or the change of the magnetization due to the applied electric field, at θ and (180° - θ) for a certain value of φ have nearly the same magnitude but the signs are equal or opposite according to the direction of the electric field and the pick up coil, as tabulated in Table 3-II. Difference in the magnitude of the output for θ and 180° - θ was composed of two parts: the intrinsic one and the leakage of other signals. (See Fig. 3-8.) The former, the part corresponding to the breaking of the monoclinic symmetry, was so small that it could not be subjected to a quantitative discussion. We will confine ourselves to the monoclinic part.

The output was proportional to the applied voltage up to 55V, within the accuracy of the experiment. The effect quadratic in E could not be separated, though the magnetic field dependence of the electric susceptibility (see Sec. 3-3-4) indicated its existence.

Table 3-II Character of the signal with the mirror symmetry parallel to $(1\bar{1}0)$, corresponding to the direction of the electric field and the axis of the pick up coil.

E / δM	[111]	[11$\bar{2}$]	[1$\bar{1}$0]
[111]	Symmetric	Symmetric	Antisymmetric
[11$\bar{2}$]	Symmetric	Symmetric	Antisymmetric
[1$\bar{1}$0]	Antisymmetric	Antisymmetric	Symmetric

Symmetric: signal(180° - θ) = signal(θ)

Antisymmetric: signal(180° - θ) = - signal(θ).

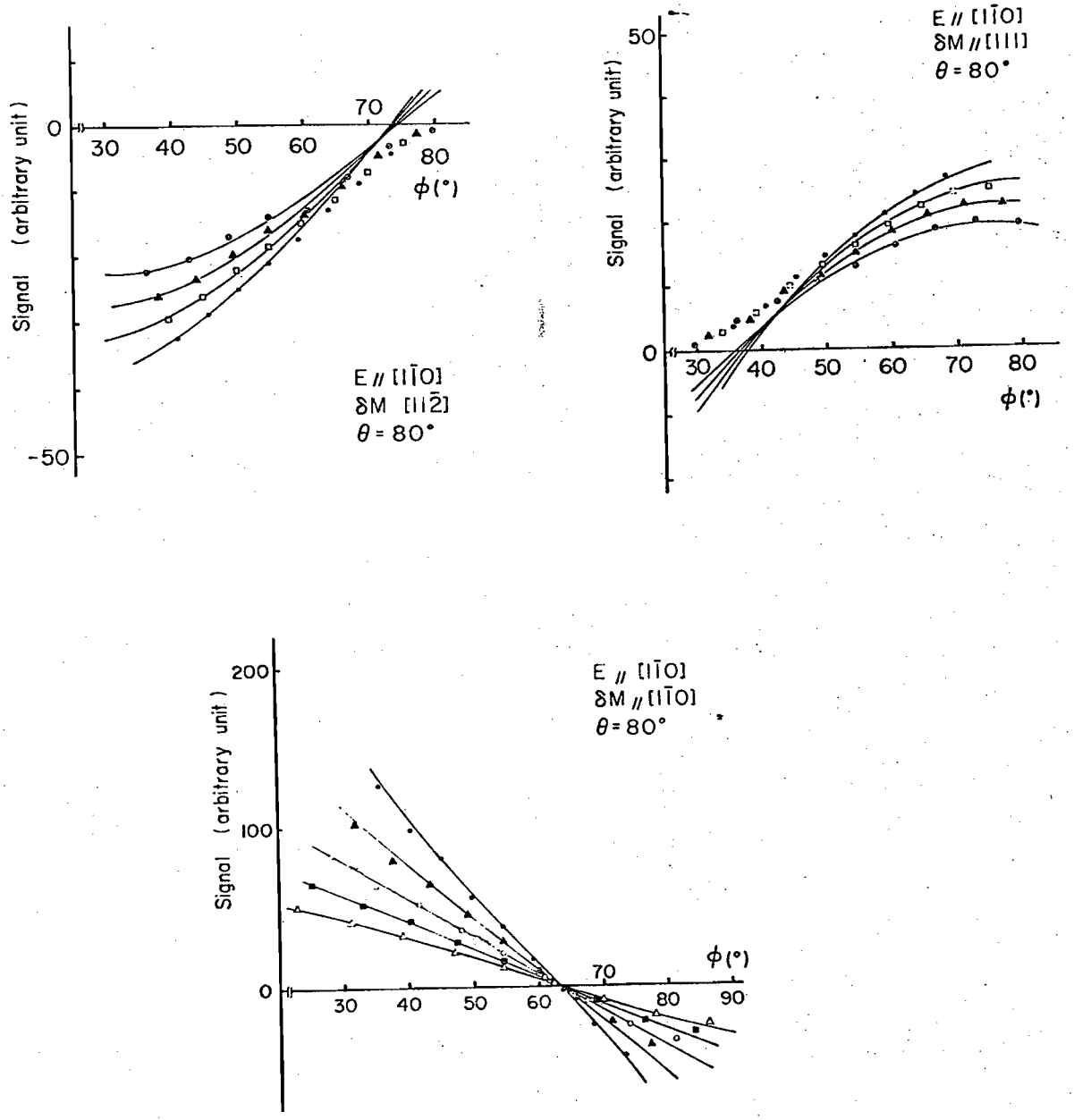

Fig. 3-10 Experimentally determined ME signal with monoclinic symmetry, in the case of E // [1$\bar{1}$0] and θ = 80°. External magnetic field was 8.4 kOe (●), 10 kOe (□), 12 kOe (▲), 15 kOe (⊘), 17 kOe (○), 23.3 kOe (▣) or 31.4 kOe (△). Solid lines are calculated for the rotation mechanism.

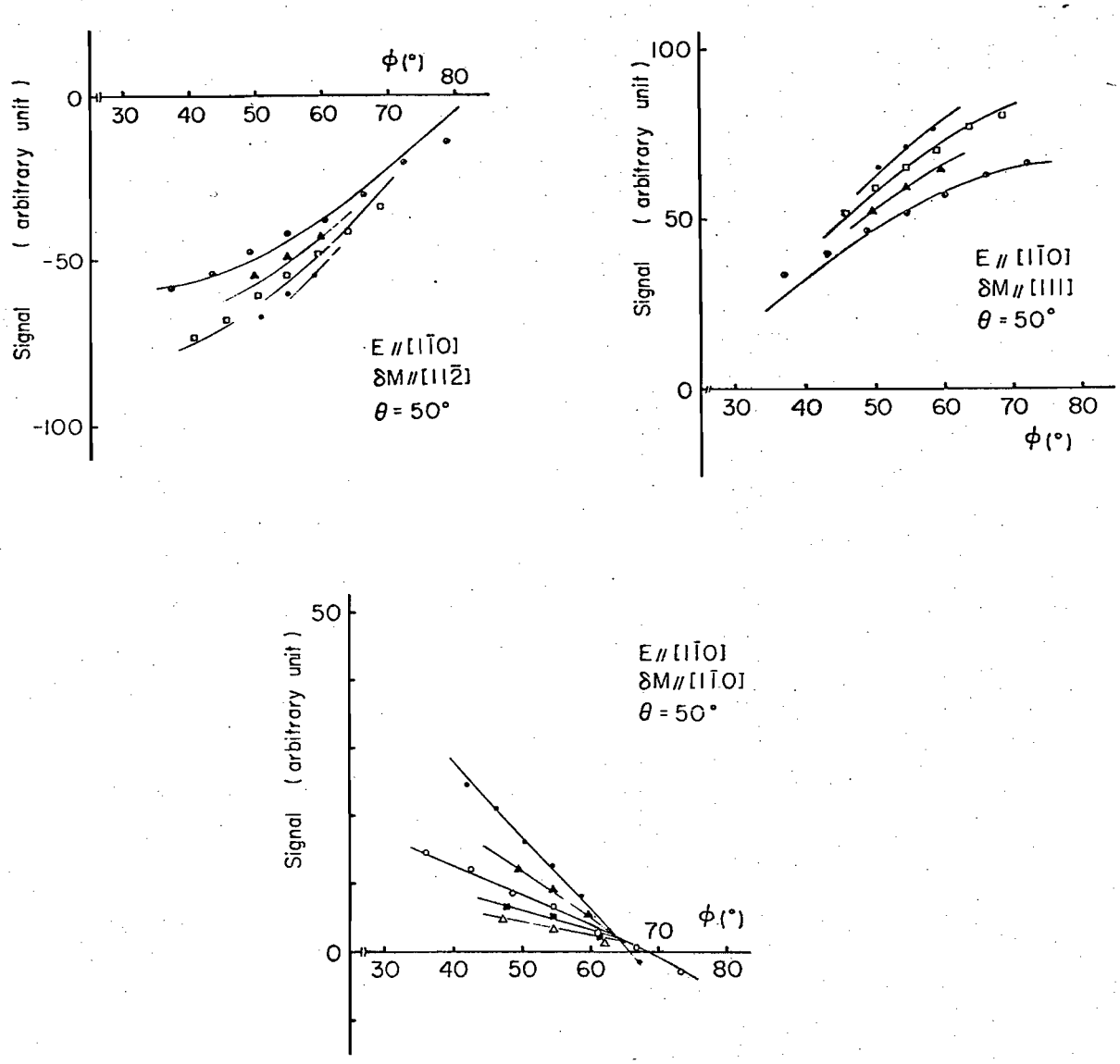

Fig. 3-11 Experimentally determined ME signal with monoclinic symmetry, in the case of E // [1$\bar{1}$0] and θ = 50°
Solid curves are calculated for the rotation mechanism.

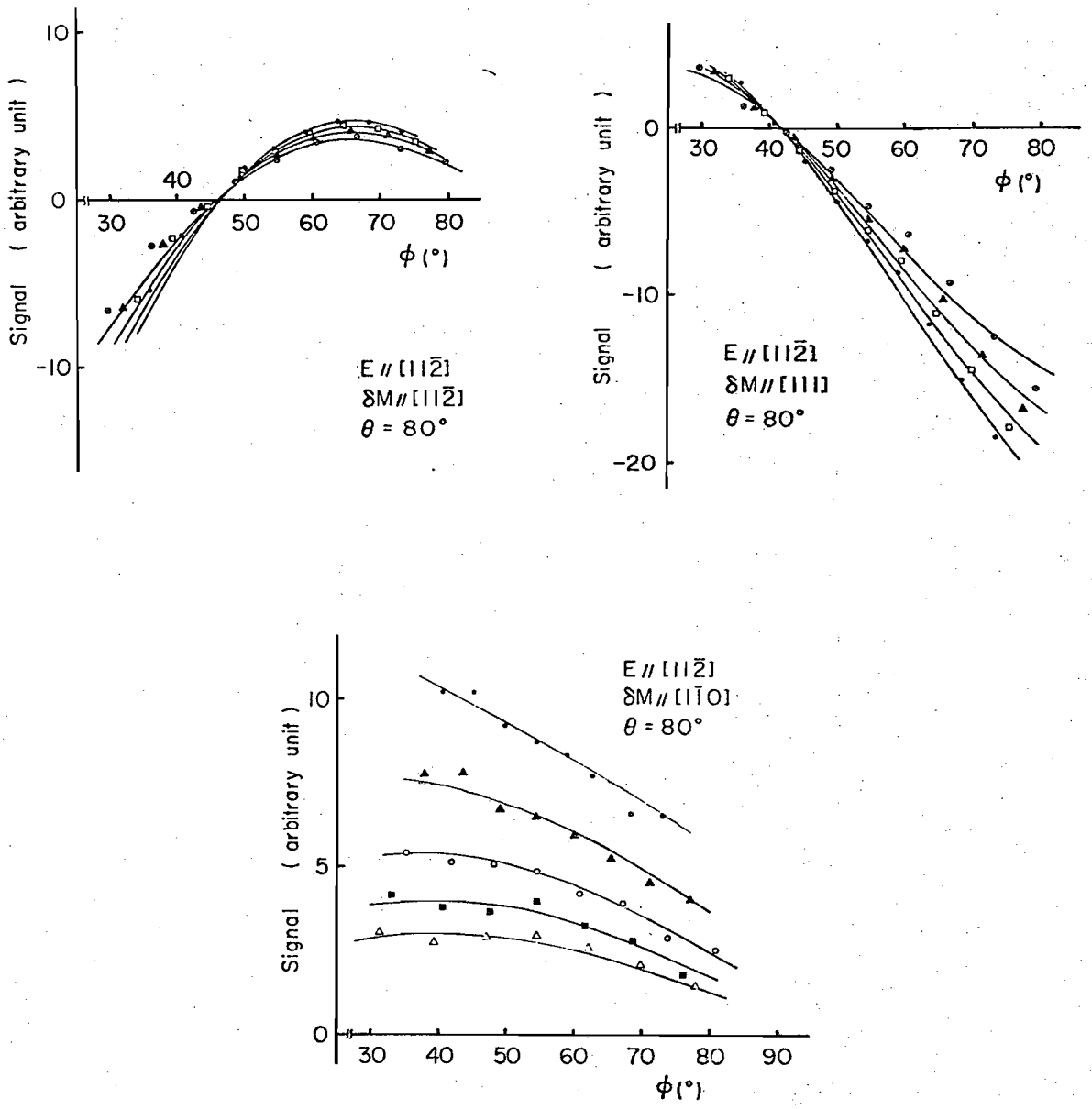

Fig. 3-12 Experimentally determined ME signal with monoclinic symmetry, in the case of E // [11$\bar{2}$] and θ = 80°
Solid curves are calculated for the rotation mechanism.

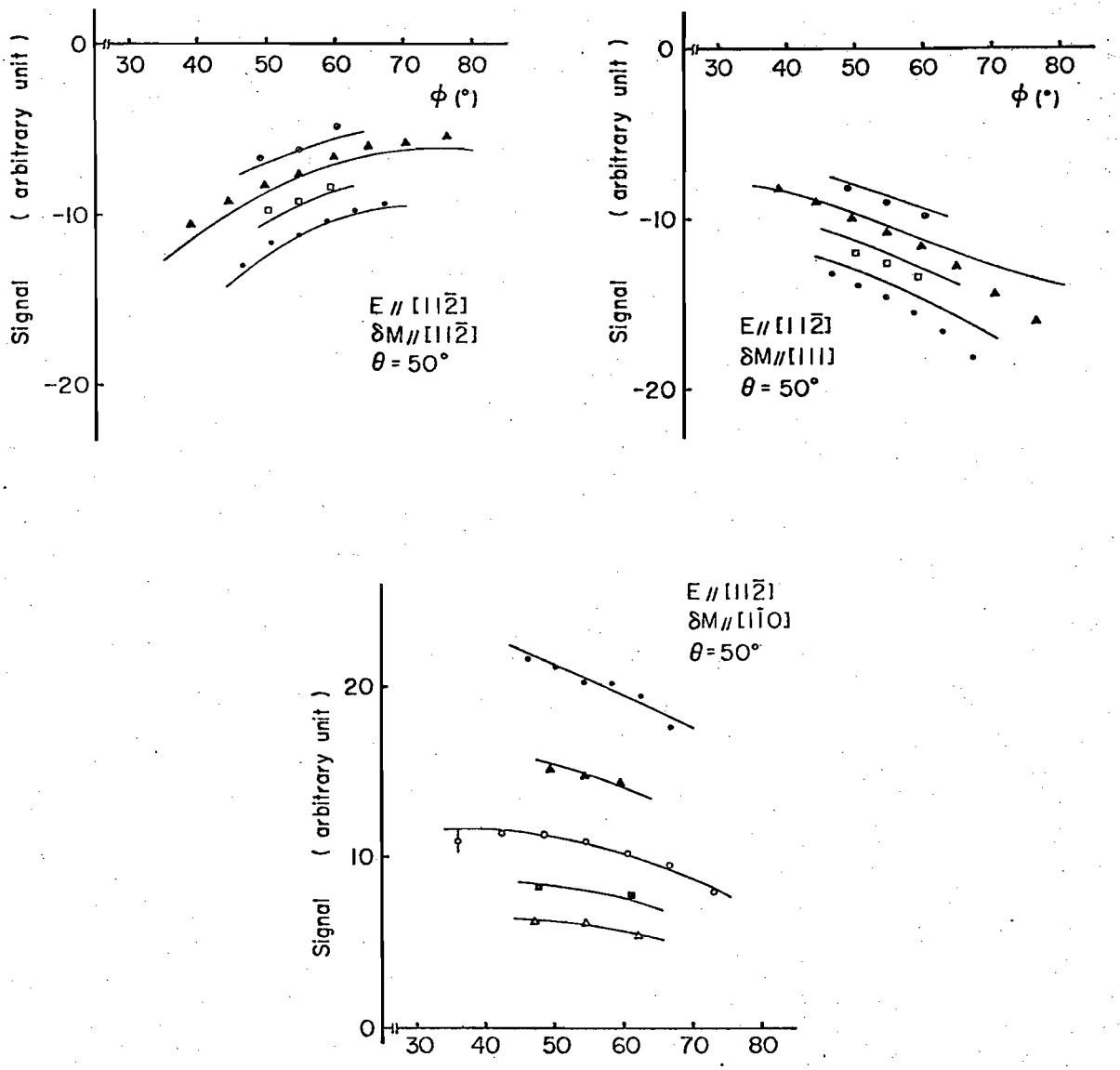

Fig. 3-13 Experimentally determined ME signal with monoclinic symmetry, in the case of E // [11$\bar{2}$] and θ = 50°
Solid curves are calculated for the rotation mechanism.

Examples of the monoclinic part of the output are shown in Figs. 3-10 ∿ 13 for several values of θ. The signal for an arbitrary φ was determined by the interpolation of the experimental points.

According to the tilting of the magnetization from its equilibrium position, Zeeman and crystalline anisotropy energy, ε^o in eq. (3-2), increases as a quadratic function of the tilting angle.

$$\delta\varepsilon^o = \frac{1}{2}\varepsilon^o_{\theta\theta}\delta\theta^2 + \varepsilon^o_{\theta\phi'}\delta\theta\delta\phi' + \frac{1}{2}\varepsilon^o_{\phi'\phi'}\delta\phi'^2. \qquad (3\text{-}3)$$

Here, $\delta\theta$ and $\delta\phi'$ are tilting angles of the magnetization along two great circles perpendicular with each other and crosses at the equilibrium position. Note that the circle with constant θ is not the great circle and φ is not the coordinate. (See Fig. 3-14.) $\varepsilon^o_{\theta\theta}$, $\varepsilon^o_{\theta\phi'}$ and $\varepsilon^o_{\phi'\phi'}$ can be calculated from eq.(3-2) for any (θ, φ) and H.

In general, the part of the magnetic anisotropy energy proportional to the electric field, ε^{ME}, has linear terms of $\delta\theta$ and $\delta\phi'$. The deviations of the magnetization from the equilibrium position are determined by the following equations:

$$\begin{aligned}\frac{\partial}{\partial\theta}\varepsilon &= \frac{\partial}{\partial\theta}(\varepsilon^o + \varepsilon^{ME}) = \varepsilon^o_{\theta\theta}\,\delta\theta + \varepsilon^o_{\theta\phi'}\,\delta\phi' + \varepsilon^{ME}_{\theta} = 0,\\ \frac{\partial}{\partial\phi'}\varepsilon &= \frac{\partial}{\partial\phi'}(\varepsilon^o + \varepsilon^{ME}) = \varepsilon^o_{\theta\phi'}\delta\theta + \varepsilon^o_{\phi'\phi'}\delta\phi' + \varepsilon^{ME}_{\phi'} = 0.\end{aligned} \qquad (3\text{-}4)$$

The form of ε^{ME} depends on the direction of the electric field.

When the direction cosines of the axis of the pick up coil with respect to our coordinate axes are α, β and γ, signal is

$$S_{\alpha\beta\gamma} = \delta M_{\alpha\beta\gamma} + (\alpha\cos\theta\cos\phi + \beta\cos\theta\sin\phi - \gamma\sin\theta)\cdot M\delta\theta + (-\alpha\sin\phi + \beta\cos\phi)\cdot M\delta\phi'. \tag{3-5}$$

Here, δM is the signal due to the change in the magnitude of the magnetization without tilting of the spins (non-rotation part) and the remaining terms are those due to the rotation (rotation part). Then, for the cases of $[1\bar{1}0]$, $[11\bar{2}]$ and $[111]$ pick up,

$$\begin{aligned} S_{1\bar{1}0} &= \delta M_{1\bar{1}0} - \sin\theta\, M\delta\theta, \\ S_{11\bar{2}} &= \delta M_{11\bar{2}} + \cos\theta\sin\phi\, M\delta\theta + \cos\phi\, M\delta\phi', \\ S_{111} &= \delta M_{111} + \cos\theta\cos\phi\, M\delta\theta - \sin\phi\, M\delta\phi'. \end{aligned} \tag{3-6}$$

When the magnetization lies in the $(1\bar{1}0)$ plane, $\varepsilon^{o}_{\theta\phi'}$ is equal to 0 because of the mirror symmetry and $\delta\theta$ and $\delta\phi'$ are expressed simply,

$$\begin{aligned} \delta\theta &= -\varepsilon^{ME}_{\theta}/\varepsilon^{o}_{\theta\theta}, \\ \delta\phi' &= -\varepsilon^{ME}_{\phi}/\varepsilon^{o}_{\phi'\phi'}. \end{aligned} \tag{3-7}$$

As $\cos\theta = 0$ in this case, $S_{1\bar{1}0}$ plotted aginst $(\varepsilon^{o}_{\theta\theta})^{-1}$ and $S_{11\bar{2}}$ or S_{111} plotted against $(\varepsilon^{o}_{\phi'\phi'})^{-1}$ should lie on a straight line. The slope gives $\varepsilon^{ME}_{\theta}$ and $\varepsilon^{ME}_{\phi'}$, multiplied by $\sin\theta$ (= 1), $\cos\phi$ or $\sin\phi$, and the extrapolation of the line gives δM as the intersection with the coordinate axis. When the magnetization is near (110) plane, i.e., $\phi \simeq 55°$, $\varepsilon^{o}_{\theta\phi'}$ is small and can be

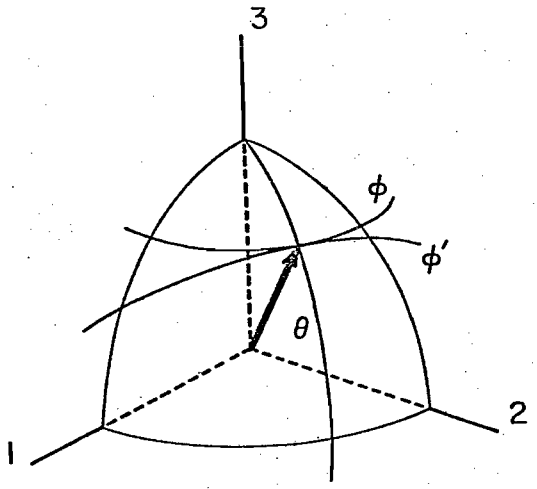

Fig. 3-14 Coordinates on a spherical surface, θ, ϕ' and ϕ.

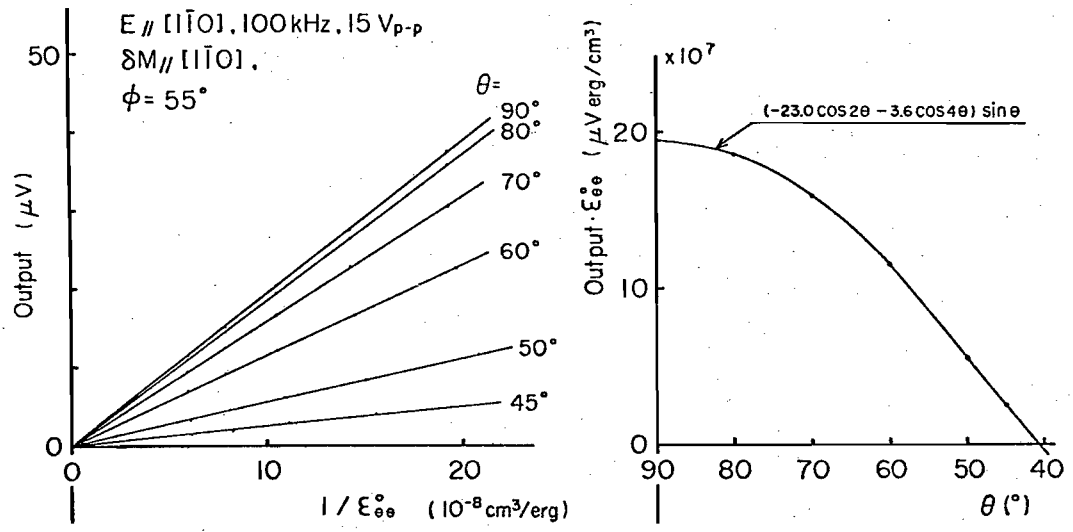

Fig. 3-15 Plot of the output against the inverse of the curvature of ε^{o} along θ, in the case of E // [1$\bar{1}$0] and Φ = 0°

neglected in eq.(3-5). In this case, however, separation of signals into the rotation and non-rotation parts is possible only for $S_{1\bar{1}0}$, as $S_{11\bar{2}}$ and S_{111} have both $\delta\theta$ and $\delta\phi'$ terms. An example of separation of these two parts is shown in Fig. 3-15. In all cases where the plot as in Fig. 3-15 is possible, it was confirmed that the δM term is small compared with the $\delta\theta$ or $\delta\phi'$ terms. We can thus conclude that the rotation of the magnetization is the main origin of the ME effect in Fe_3O_4 at 77 K.

In the following, analysis of ε^{ME} will be reported for the electric field parallel to $[1\bar{1}0]$ and $[11\bar{2}]$. In the case of (111) electrodes, the output was too small and its reproducibility was too poor to be quantitatively analyzed. (See Sec. 3-3-4.)

A $E \parallel [1\bar{1}0]$.

Since the electric field is perpendicular to the mirror plane in this case, only the terms antisymmetric to $(1\bar{1}0)$ appear in the expression of ε^{ME}. Spherical harmonics expansion of ε^{ME} gives

$$\begin{aligned}\varepsilon^{ME}_{1\bar{1}0} = E_{1\bar{1}0} [\, & a' \cos\theta\sin\theta\sin\Phi + b' \cos\theta\sin\theta\cos\Phi \\ & + c' \cos^3\theta\sin\theta\sin\Phi + d' \cos^3\theta\sin\theta\cos\Phi \\ & + e' \cos\theta\sin^3\theta\sin 3\Phi + f' \cos\theta\sin^3\theta\cos 3\Phi \\ & + \cdots\cdots \qquad\qquad], \end{aligned} \tag{3-8}$$

where $\Phi = \phi - 55°$. Hereafter, we will confine ourselves to the spherical harmonics up to the fourth order. Then,

$$\varepsilon_{\theta}^{ME} = E_{1\bar{1}0}\,[\{a'\sin\Phi + b'\cos\Phi + \tfrac{1}{2}(c'\sin\Phi + d'\cos\Phi + e'\sin 3\Phi + f'\cos 3\Phi)\}\cos 2\theta + \tfrac{1}{2}(c'\sin\Phi + d'\cos\Phi + e'\sin 3\Phi - f'\cos 3\Phi)\cos 4\theta],$$

$$\varepsilon_{\phi'}^{ME} = E_{1\bar{1}0}\,[a'\cos\Phi - b'\sin\Phi + c'\cos^2\theta\cos\Phi - d'\cos^2\theta\sin\Phi + 3e'\sin^2\theta\cos 3\Phi - 3f'\sin^2\theta\sin 3\Phi]\cdot\cos\theta. \qquad (3\text{-}9)$$

The problem is to determine six parameters, a' - f'. The process was as follows.

(i) θ dependence of $S_{1\bar{1}0}^{rot}$ at $\Phi = 0°$ ($\phi = 55°$) gives

$$b' + \frac{1}{2}(d' + f') = -\,112.5\ (\pm 5) \times 10^{-3}\ \ erg/cm^3/V/cm,$$
$$\frac{1}{2}(d' - f') = -\,17.5\ (\pm 3) \times 10^{-3}\ \ erg/cm^3/V/cm.$$

(See Fig. 3-15.) $\delta M_{1\bar{1}0}$ was zero in this case.

(ii) Φ dependence of $S_{1\bar{1}0}^{rot}$ for $\theta = 90°$, deduced from a similar plot as Fig. 3-15, gives

$$b' = -\,102\ (\pm 5) \times 10^{-3},$$
$$f' = \quad 7\ (\pm 2) \times 10^{-3},$$
$$a' + 3e' = 650\ (\pm 15) \times 10^{-3},$$

all in the unit of $erg/cm^3/V/cm$. Since the variable range of Φ in our experiment was only $\pm 30°$, where $\sin 3\Phi$ is nearly equal to $3\sin\Phi$, a' and e' could not be determined separately. In this case, also, $\delta M_{1\bar{1}0}$ was nearly zero.

Above four conditions on b', d' and f' give

$$b' = -100 \pm 5 \times 10^{-3} \text{ erg/cm}^3\text{/V/cm},$$

$$d' = -27 \pm 5 \times 10^{-3},$$

$$f' = 7 \pm 2 \times 10^{-3}.$$

(iii) From the θ dependence of S_{111} and $S_{11\bar{2}}$ for $\Phi = 0$, $c' - 3e'$, was estimated as -95 ± 10 erg/cm^3/kV/cm on an assumption of vanishing δM_{111} and $\delta M_{11\bar{2}}$.

We have only two conditions so far on a', c' and e'. They were determined by the comparison of the calculated S^{rot} with the measured value in the whole range of θ and ϕ where the experiment was carried out. Though a', c' and e' giving the same value for $a' + 3e'$ and $c' - 3e'$ resulted in similar curves, overall fitting was best for the following values.

$$a' = 460 \pm 70 \times 10^{-3} \text{ erg/cm}^3\text{/V/cm},$$

$$c' = 120 \pm 70 \times 10^{-3},$$

$$e' = 75 \pm 20 \times 10^{-3}.$$

Note that $\pm$ for a', c' and e' in eq.(3-11) are not independent with each other.

Solid lines in Figs. 3-10 and 3-11 are calculated with these values. As a whole, agreement of experimental points and calculated curves is good, except S_{111} for lower values of ϕ and $S_{11\bar{2}}$ for higher values of ϕ. Since the signals for these values of ϕ picked up along other directions are well reproduced by the calculation, this discrepancy can not be caused by the error in ε^o. Leakage of $S_{1\bar{1}0}$ is also eliminated as $S_{1\bar{1}0}$ is

symmetric whereas S_{111} and $S_{11\bar{2}}$ are antisymmetric. (See Table 3-II.) The discrepancy at $\theta = 70°$ was nearly twice of that at $\theta = 80°$: nearly proportional to the b component of the magnetization for the small value of $\theta - 90°$. A possible origin of the discrepancy is the δM terms in eq.(3-6).

B $E \parallel [11\bar{2}]$.

In this case, electric field does not break the mirror symmetry and ε^{ME} is symmetric to the b plane.

$$\varepsilon^{ME}_{11\bar{2}} = E_{11\bar{2}} [a \cos^2\theta + b \sin^2\theta\sin2\Phi + c \sin^2\theta\cos2\Phi + d \cos^4\theta + e \cos^2\theta\sin^2\theta\sin2\Phi + f \cos^2\theta\sin^2\theta\cos2\Phi + g \sin^4\theta\sin4\Phi + h \sin^4\theta\cos4\Phi]. \quad (3\text{-}12)$$

and

$$\varepsilon^{ME}_{\theta} = E_{11\bar{2}} [(-a - d + b\sin2\Phi + c\cos2\Phi + g\sin4\Phi + h\cos4\Phi)\sin2\theta + \tfrac{1}{2}(-d + e\sin2\Phi + f\cos2\Phi - g\sin4\Phi - h\cos4\Phi)\sin4\theta$$
$$\varepsilon^{ME}_{\phi'} = E_{11\bar{2}} [2(b + e\cos^2\theta)\cos2\Phi - 2(c + f\cos^2\theta)\sin2\Phi + 4g \sin^2\theta\cos4\Phi - 4h \sin^2\theta\sin4\Phi] \sin\theta. \quad (3\text{-}13)$$

Now, eight, instead of six, parameters are to be determined. After a process essentially same as above but much more tiresome, parameters were determined as follows:

$$a = 100 \pm 15 \times 10^{-3} \quad \text{erg/cm}^3\text{/V/cm},$$
$$c = -147 \pm 15 \times 10^{-3}, \qquad b = 66 \pm 4 \times 10^{-3},$$
$$d = 32 \pm 10 \times 10^{-3},$$
$$f = 34 \pm 20 \times 10^{-3}, \qquad e = -27 \pm 4 \times 10^{-3}, \quad (3\text{-}14)$$
$$h = -14 \pm 10 \times 10^{-3}, \qquad g = 9 \pm 2 \times 10^{-3}.$$

Again, ± for a, c, d, f and h are not independent.

Solid curves in Figs. 3-12 and 3-13 were calculated with these values. Agreement between the calculated and observed values is less well than the case of $\vec{E} \parallel [1\bar{1}0]$, though the characteristic features of the anisotropy is reproduced. $\delta M_{1\bar{1}0}$ seems absent in the whole range. For $\Phi = 0°$, this was proved by a plot as in Fig. 3-15. On the contrary, δM_{111} and $\delta M_{11\bar{2}}$ appeared in the b plane, at higher angles of ϕ for the former and at lower angles for the latter, and seems to decrease rather slowly with decreasing θ from 90°.

3-3-3 Relaxation of the ME effect

When the frequency of the applied voltage was increased, magnitude of the signal increased but not so much as is expected from the increase of the pick up efficiency. Fig. 3-16 shows the frequency dependence of the ME output, normalized at the value extrapolated to 0 Hz. Again, E and δM were both parallel to $[1\bar{1}0]$ in this case and the magnetization was set parallel to [001]. The frequency dependence can be explained by the equation:

$$y = C/(1 + \omega^2 \tau_o^2), \qquad (3\text{-}15)$$

if τ_o is assumed 2 μsec. Similar frequency dependence was observed for other directions of E and δM, and for a specimen with different dimension (2.3 mm cube).

Relaxation in the ME effect can originate from electric and/or magnetic relaxation. If the coupling is through the

acoustic phonons (electric field - electrostriction - strain - magnetostriction - change in magnetization), size of the sample can also affect the response. The third possibility is rejected, however, since the same relaxation time within the experimental error was observed in a smaller sample.

2 μsec seems rather long for a relaxation time of an electron system at 77 K. Galt had reported a relaxation time of approximately 50 μsec in polycrystalline Fe_3O_4 at room temperature by the initial permeability measurement.[19] He attributed this to the relaxation in the magnetic domain wall motion. On the other hand, dispersion in the dielectric properties of Fe_3O_4 or γ-Fe_2O_3 fine particles at low temperatures was reported.[20] This was explained by the inhomogeneity of the sample. The phenomenon shown in Fig. 3-16 does not seem to be correlated to these two reports. Measurement of the temperature dependence of the relaxation time would be interesting and important.

3-3-4 Electric susceptibility

To make clear whether the relaxation in the ME effect has a magnetic or an electric origin, we tried to measure the electric susceptibility of Fe_3O_4 at 77 K.

Another problem that should be pointed here is the anisotropy of the ME effect in the efficiency of the electric field direction. When the ac electric field was applied along [111] direction, the output was smaller by approximately one order of magnitude, compared with the results for $[1\bar{1}0]$ or $[11\bar{2}]$ direction of the electric field. The reproducibility was poor by the change of

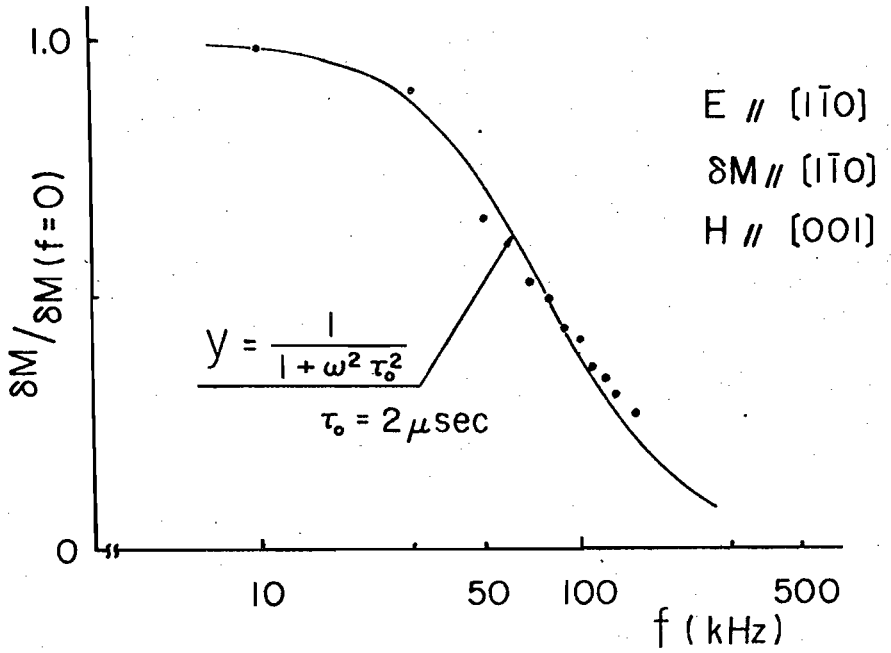

Fig. 3-16 Frequency dependence of the ME effect, normalized at the low frequency limit. Solid line shows the dependence with a single relaxation time of 2 μsec.

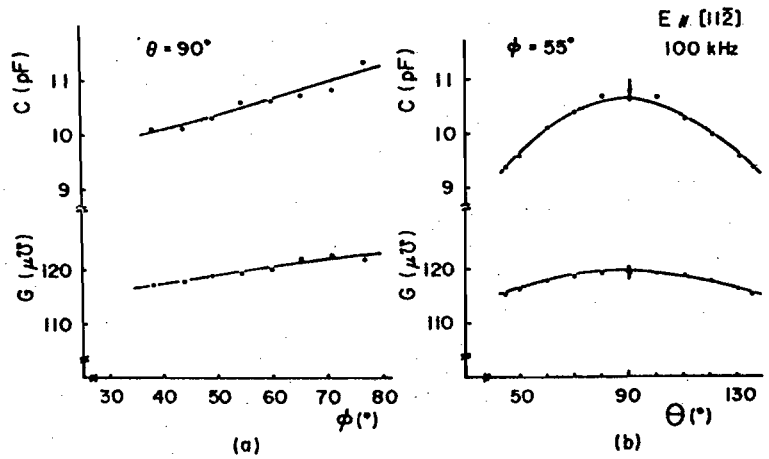

Fig. 3-17 Capacitance and conductance along [11$\bar{2}$], as a function of the magnetization direction. The frequency was 100 kHz.

the sample setting. This was supposed to be due to the leakage of signals by the non-parallel component of the electric field. Tilting of the magnetization direction during the poling had little effect, in contrast to the case of $(1\bar{1}0)$ electrodes, and the perpendicular orientation of the pulsed dc electric field to the electric polarization cannot be the cause. This suggests the anisotropy in the electric susceptibility, or the relation between $\vec{E}$ and $\vec{P}$.

At the same time, if the terms quadratic in $\vec{E}$ and linear or quadratic in $\vec{M}$ exist in the expression of the free energy, they will reflect in the dependence of the electric susceptibility on the direction of the magnetization.

As was mentioned in Sec. 3-2-4, high electrical conductivity of Fe_3O_4 prevented precise measurement of ε at 77 K. An example of the results measured at 100 kHz is shown in Fig. 3-17, as a function of the magnetization direction. To have ε', the real part of the complex susceptibility, the capacitance in pF should be multiplied by approximately 20 in this case. When measured along [111] or $[1\bar{1}0]$, capacitance was almost constant for changing θ, ϕ being kept 55°. ϕ dependence for $\theta = 90°$ was similar to Fig. 3-17. Capacitance along [111] was smaller than those along $[11\bar{2}]$ or $[1\bar{1}0]$ by about half an order of magnitude.

At lower frequencies, 1 or 10 kHz, the capacitance was much larger than those at 100 kHz but the conductance was nearly the same. However, the reproducibility of the measurement at these frequencies was poor and we could not have reliable data. On

the contrary, capacitance was so small at 1 MHz and the bridge could not be balanced. Qualitatively, a large dispersion in ε was evident and we suppose that the relaxation in the ME effect shown in Fig. 3-16 has electrical origin. Here again, temperature dependence is interesting, though the measurement will be difficult at temperatures higher than 77 K. Small ME coefficient for the electric field along the [111] axis seems also to be attributed to the small ε along this direction.

Dependence of ε on the direction of the magnetization shows the existence of the ME free energy term quadratic in $\vec{E}$. Strength of the external magnetic field or even the reversal of the magnetization direction did not affect the capacitance, and the term should be even powers in $\vec{M}$.

§ 3-4 Discussion

3-4-1 Electric field dependence of the magnetic anisotropy

In the last section, it was disclosed that the ME effect of Fe_3O_4 at 77 K is mainly due to the rotation of spins, though the non-rotation mechanism could not be totally excluded. The non-rotation terms, δM, were too small to be analyzed quantitatively. As for the rotation terms, magnitude of the parameters given in Sec. 3-3-2 should be considered tentative, since we have no direct evidence for the saturation of the electric polarization by the ME poling. However, considering the reproducibility of the experimental results, we believe that these values are not much smaller than the proper ones. At any rate, relationships between a', ··· , f' or a, ··· , h are correctly given.

To interpret these parameters, we will assume that the magnetic anisotropy depending on the electric polarization, $\vec{P}$, is small compared with the total anisotropy and is proportional to a monotonic function of P. Since we consider here only those terms consistent with the mirror symmetry, the $\vec{P}$ dependent magnetocrystalline anisotropy energy can be expanded as follows:

$$\begin{aligned}\varepsilon_A^{ME} = {} & K_{20}\alpha_b^2 - 2K_{22s}\alpha_a\alpha_c - K_{22c}(\alpha_a^2 - \alpha_c^2) \\ & + K_{40}\alpha_b^4 - 2K_{42s}\alpha_b^2\alpha_a\alpha_c - K_{42c}\alpha_b^2(\alpha_a^2 - \alpha_c^2) \\ & + 4K_{44s}\alpha_a\alpha_c(\alpha_a^2 - \alpha_c^2) + K_{44c}(\alpha_a^4 - 6\alpha_a^2\alpha_c^2 + \alpha_c^4). \qquad (3\text{-}16)\end{aligned}$$

α_c, α_b and α_a are the direction cosines of the magnetization with respect to [001], [1$\bar{1}$0] and [110] axes, respectively (see Fig. 3-2), and the terms sixth or higher order spherical harmonics were neglected.[13] The electric polarization connected to this anisotropy is parallel to the b plane, when the magnetization lies in the same plane.

Application of the external electric field along [1$\bar{1}$0], the b axis, rotates $\vec{P}$ without the change of its magnitude, and thus results in the rotation of the principal axes of ε_A^{ME} out of the b plane, without the change of the magnitude of K's. If we denote the small rotation of the axes around [110] axis by δa and that around [001] axis by δc,

$$\begin{aligned}
\varepsilon_{1\bar{1}0}^{ME} = {} & [(-2K_{20}+2K_{22c}-K_{42c})\delta c - (2K_{22s}-K_{42s})\delta a]\sin\theta\cos\theta\sin\Phi \\
& + [-(2K_{22s}-K_{42s})\delta c - (2K_{20}+2K_{22c}-K_{42c})\delta a]\sin\theta\cos\theta\cos\Phi \\
& + [(-4K_{40}+3K_{42c})\delta c - 3K_{42s}\delta a]\cos^3\theta\sin\theta\sin\Phi \\
& + [-3K_{42s}\delta c - (4K_{40}+3K_{42c})\delta a]\cos^3\theta\sin\theta\cos\Phi \\
& + [(K_{42c}-4K_{44c})\delta c + (K_{42s}+4K_{44s})\delta a]\cos\theta\sin^3\theta\sin 3\Phi \\
& + [(-K_{42s}+4K_{44s})\delta c + (K_{42c}+4K_{44c})\delta a]\cos\theta\sin^3\theta\cos 3\Phi . \qquad (3\text{-}17)
\end{aligned}$$

On the contrary, if the electric field is applied along [11$\bar{2}$], parallel to the b plane, the electric polarization changes its magnitude and is rotated around the b axis. Then,

$$\varepsilon^{ME}_{11\bar{2}} = \delta K_{20}\cos^2\theta - (\delta K_{22s}+2K_{22c}\delta b)\sin^2\theta\sin 2\Phi$$
$$- (\delta K_{22c}-2K_{22s}\delta b)\sin^2\theta\cos 2\Phi$$
$$+ \delta K_{40}\cos^4\theta - (\delta K_{42c}+2K_{42c}\delta b)\cos^2\theta\sin^2\theta\sin 2\Phi$$
$$- (\delta K_{42c}-2K_{42s}\delta b)\cos^2\theta\sin^2\theta\cos 2\Phi$$
$$+ (\delta K_{44s}+4K_{44c}\delta b)\sin^4\theta\sin 4\Phi$$
$$+ (\delta K_{44c}+4K_{44s}\delta b)\sin^4\theta\sin 4\Phi. \quad (3\text{-}18)$$

Here, δK's are the change of the anisotropy constants and δb is the rotation angle of the principal axes of ε^{ME}_{A} around the b axis.

There are 19 unkown parameters in eqs.(3-17) and (3-18), eight K's, eight δK's, δa, δb and δc. On the above assumption between P and ε^{ME}_{A}, however, K's are determined by P and δK's are proportional to δP and $(K/\delta K)$'s, determined by $P/\delta P$, are constant. If we define new parameters, $A = \delta a \cdot K/\delta K$, $B = \delta b \cdot K/\delta K$ and $C = \delta c \cdot K/\delta K$, the number of independent parameters are decreased to eleven: eight δK's, A, B and C. These parameters were determined from the condition that the sum of the difference between calculated and experimentally determined a - h and a' - f' should be minimum. There are two minimal points with almost the same value of the difference and the two sets of parameter values are shown in Table 3-III. In both cases, fourth order terms are much smaller than the second order terms. 100 erg/cm^3/kV/cm corresponds to 1.3×10^{-4} cm^{-1}/Fe_3O_4/kV/cm and should be compared

Table 3-III Electric field dependence of the magnetocrystalline anisotropy constants ($erg/cm^3/kV/cm$)

	Case 1	Case 2
δK_{20}	100 ± 10	105 ± 10
δK_{22s}	45 ± 5	- 90 ± 5
δK_{22c}	40 ± 8	18 ± 5
δK_{40}	- 5 ± 3	- 9 ± 3
δK_{42s}	- 6 ± 3	12 ± 3
δK_{42c}	- 9 ± 3	- 5 ± 2
δK_{44s}	- 2 ± 2	2 ± 1
δK_{44c}	1 ± 1	3 ± 1
$A = \delta aK/\delta K$	2.4 ± 0.5	- 12.5 ± 2
$B = \delta bK/\delta K$	- 1.4 ± 0.4	0.7 ± 0.2
$C = \delta cK/\delta K$	- 6.5 ± 0.4	- 17 ± 1
ϕ of the electric polarization	- 15 ± 5°	109 ± 5°
ϕ of the principal axes of ε_A^{ME} in the b plane	- 11 ± 5°	106 ± 5°
	79 ± 5°	16 ± 5°

with 1.1×10^{-6} $cm^{-1}/Cr^{3+}/kV/cm$ for Cr_2O_3 at 4.2 K (see Sec. 2-3-3) or 9×10^{-6} $cm^{-1}/kV/cm$ for ruby at the room temperature.[21] The electric susceptibility of Fe_3O_4 at 77 K is approximately 50 times larger than that of Cr_2O_3 (see Sec. 3-3-4) and the electric polarization dependence of the magnetic anisotropy energy is almost the same. Considering the large difference in the total anisotropy energy, ME effect in Fe_3O_4 is weaker than that in Cr_2O_3.

By the electric field applied along the b axis, $\vec{P}$ will tilt to the b axis, or rotate around the axis perpendicular to both $\vec{P}$ and the b axis. Then, the azimuthal angle of $\vec{P}$, Φ_p, can be estimated by $\tan^{-1}(C/A)$. On the other hand, the principal axes of the second order anisotropy is determined from K_{22s} and K_{22c}. These angles are also shown in Table 3-III. In both case 1 and case 2, one of the principal axes of ε_A^{ME} coincides with the direction of the electric polarization within the experimental error. If we take a Cartesian coordinate (ξ, η, ζ), where ζ is along the direction of the electric polarization and η is parallel to the b axis, the second order terms in ε_A^{ME} are expressed as

$$-140\alpha_\zeta^2 + 20(\alpha_\xi^2 - \alpha_\eta^2) \quad (erg/cm^3/kV/cm) \text{ for the case 1,}$$

and

$$-190\alpha_\zeta^2 + 10(\alpha_\xi^2 - \alpha_\eta^2) \quad \text{for the case 2,}$$

where α_i is the direction cosine of the magnetization to the axis i. Here, let us try the order estimation of ε_A^{ME}. In the

present approximation, the magnitude depends on the electric polarization. If this is 1 $\mu C/cm^2$, for example, K's are approximately 3 times as big as δK's for 1 kV/cm of the external electric field, since the electric susceptibilities along $[1\bar{1}0]$ and $[11\bar{2}]$ were about 500 (see Sec. 3-3-4). Then, the magnetic anisotropy energy accompanied by the electric polarization is the order of 10^3 erg/cm^3. This small value strongly suggests that the ME effect does not play a primary role in the phase transition of Fe_3O_4 at T_v but only a secondary one. At the same time, this supports our assumption of small ε_A^{ME} and the calculation of ε^o from the data of Abe et al.[13], where no poling was performed on the specimen.

The assumed ratio of 3 for K/δK gives the tilting angle of the principal axes of ε_A^{ME}, δa etc., up to 2×10^{-3} radian/kV/cm (case 1) or 5×10^{-3} (case 2). In the case of ruby at 300 K, the tilting of the spin axis due to the electric field perpendicular to the c axis was estimated as 1.6×10^{-5} radian/kV/cm.[21] The difference of the electric susceptibility being taken into account, the tilting angle is almost the same for Fe_3O_4 and ruby.

3-4-2 Low temperature phase of Fe_3O_4 and the character of phase transition

In Sec. 3-3-1, it was disclosed that the low temperature phase of magnetite is triclinic at 77 K. However, the breaking of mirror symmetry is much smaller than the breaking of inversion or two-fold rotation. This was concluded from the fact that the difference of the antisymmetric part in two measurements, after the ME poling

with θ larger and smaller than 90°, was only several per cent of the total signal. In reported diffraction experiments,[12,14] it seems that the existence of the (4,4,1/2) reflection with an intensity of less than several per cent of that of $(4,\bar{4},1/2)$ or the broadening of $(4,\bar{4},1/2)$ due to the splitting by the order of 0.01° has not been eliminated, and hence the present result is not necessarily inconsistent with the diffraction experiments. The smallness of the breaking of the mirror symmetry suggests that it is caused by a perturbation of some higher order interaction and, as the first order approximation, magnetite at 77 K can be considered as monoclinic.

In Sec. 3-3-2, existence of non-rotation term was reported when the applied electric field was parallel to $[11\bar{2}]$ axis and the pick up coil axis lay within the b plane. The term became larger when the angle between the magnetization and the pick up coil axis increased. This induction of the magnetization perpendicular to it <u>without</u> the rotation of spins, can not be explained in a colinear spin structure and leads to a model with two or more spin axes.

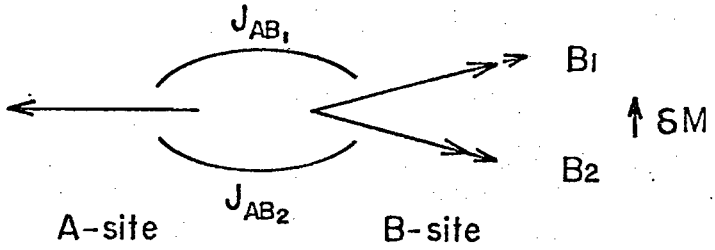

Fig. 3-18 A model of the non-rotation term. Magnetization is induced perpendicular to the direction of net magnetization.

Consider, for example, that the sublattice moment in the B site is composed of M_{B1} and M_{B2}, directions of which are little different, though both lie on the b plane. (See Fig. 3-18.) If the exchange coupling constant between the A and the B_1 sublattices (J_{AB1}) increases with the application of the electric field within the b plane whereas that between the A and the B_2 sublattices (J_{AB2}) decreases, M_{B1} increases and the total magnetic moment changes perpendicular to itself without the rotation of spins. External magnetic field does not affect this effect and this gives a mechanism of the non-rotation or δM terms in Sec. 3-3-2. This assumption of non-colinear spin structure also gives a natural explanation of the decrease of the net moment at T_v. According to the precise measurements by Umemura et al.[22] and Matsui et al.[17], magnetic moment measured along the easy axis decreases by 0.1 %: splitting of spin axis should occur in the B site. If only Fe^{2+} spins tilt without change in magnitude, the angle between two spin axes is estimated as about 2.6°.

Recently, M.Mizoguchi reported a precise experiment of the magnetic resonance of Fe^{57} nuclei in a single crystal of Fe_3O_4 at 4.2 K.[23] According to his experiment, there are five kinds of Fe^{3+} ions on the B site, four of which locate on b-lines, i.e., the nearest neighbour sequence of B sites along the b axis, and there is only one kind on a-lines. Mizoguchi analyzed his results and proposed four models of the charge ordering scheme. He argued that there might be no change in the charge ordering at the transition near 10 K, since no change was observed in NMR lines. Of his four models, No.2 has an ac glide plane perpendicular to the b axis and

is consistent with our conclusion. However, this charge ordering model has inversion center. To explain the existence of the ME effect, some other parameters for the low temperature phase, e.g., Δ_5 mode of atomic displacement, should be introduced. Large electric susceptibility and long relaxation time being considered, there is a possibility that atomic displacements corresponding to an optical phonon or the P^2M^2 term in the free energy plays some role. On the latter possibility, it should be noted that this term can be the origin of the observed ME effect.

Competition or cooperation of two different origins of the low temperature transition was already suggested in 1975 by Chikazumi[25] in connection with the temperature dependence of the critical neutron scattering[9] and that of the anomaly in the cubic magnetic anisotropy constant and the elastic constant C_{44}. One dimensional diffuse scattering of neutrons or electrons above T_v[26,27] shows a temperature dependence different from that of $(h,k,\ell+1/2)$ type critical scattering.[9] The temperature dependence of the magnetic anisotropy also suggests two kinds of order parameters below T_v.[28] The existence of the inversion center would not be a serious weak point of the model.

On the other hand, Mizoguchi's model has been received bitter complaints from diffraction experiments.[12,14] It was argued that there is a c glide, instead of an ac glide plane and the monoclinic unit cell is not primitive but base centered. However, any charge ordering model satisfying these two conditions can not explain conclusions of Mizoguchi that there is only one kind of Fe^{3+} ions

on b-lines that have a principal axis of the hyperfine field perpendicular to the a plane, if we accept his assumptions* which seems plausible. Still there is a conflict concerning the symmetry of the low temperature phase of magnetite, but the point is out of reach of the ME effect. We can only emphasize the importance of making experiments on a single crystal and the necessity of ME poling to have a single crystal of Fe_3O_4 below T_v.

---

* 1. The anisotropy of the hyperfine field at the nuclei of Fe^{3+} ions is mainly due to the magnetic dipole field produced by neighbouring cations.

2. Electron configuration on the six nearest neighbour B site determines the symmetry of the anisotropy.

3. Anderson's restriction[24]: in an tetrahedron composed of four nearest neighbour B site, there are always two Fe^{2+} and Fe^{3+} ions.

4. Equal populations of Fe^{2+} and Fe^{3+} ions on a c plane.

References

1) R.W.Millar: J. Am. Chem. Soc. 51 (1929) 215.
2) F.Okamura: Sci. Rept. Tohoku Univ. First Ser. 21 (1932) 231.
3) E.J.Verwey, P.W.Haayman and F.C.Romeijn: J. Chem. Phys. 15 (1947) 181.
4) C.H.Domenicali: Phys. Rev. 78 (1950) 458.
5) W.C.Hamilton: Phys. Rev. 110 (1958) 1050.
6) T.Yamada, K.Suzuki and S.Chikazumi: Appl. Phys. Lett. 13 (1968) 172.
7) E.J.Samuelsen, E.J.Bleeker, L.Dobrzynski and T.Riste: J. Appl. Phys. 39 (1968) 1114.
8) G.Shirane, S.Chikazumi, J.Akimitsu, K.Chiba, M.Matsui and Y.Fujii: J. Phys. Soc. Jpn. 39 (1975) 947.
9) Y.Fujii, G.Shirane and Y.Yamada: Phys. Rev. B11 (1975) 2036, Y.Yamada: AIP Conf. Proc. 24 (1974) 79.
10) G.T.Rado and J.M.Ferrari: Phys. Rev. B12 (1975) 5166, Phys. Rev. B15 (1977) 290.
11) G.Quèzel and H.Schmid: Solid State Commun. 6 (1968) 447.
12) J.Yoshida and S.Iida: J. Phys. Soc. Jpn. 42 (1977) 230.
13) K.Abe, Y.Miyamoto and S.Chikazumi: J. Phys. Soc. Jpn. 41 (1976) 1894.
14) M.Iizumi and G.Shirane: Solid State Commun. 17 (1975) 433.
15) K.Chiba, S.Chikazumi and K.Suzuki: Proc. Int. Conf. Ferrite (University of Tokyo Press, Tokyo, 1971) p.595.
16) S.Todo and S.Chikazuni: J.Phys. Soc. Jpn. 43 (1977) 1091.
17) M.Matsui, S.Todo and S.Chikazumi: J. Phys. Soc. Jpn. 43 (1977) 47.
18) T.H.O'Dell: Int. J. Magn. 4 (1973) 239.
19) J.K.Galt: Phys. Rev. 85 (1952) 664.
20) K.Iwauchi: Jpn. J. Appl. Phys. 10 (1971) 1520.
21) E.B.Royce and N.Bloembergen: Phys. Rev. 131 (1963) 1912.
22) S.Umemura amd S.Iida: J. Phys. Soc. Jpn. 40 (1976) 697.
23) M.Mizoguchi: J. Phys. Soc. Jpn. 44 (1978) 1501, 1512.
24) P.W.Anderson: Phys. Rev. 102 (1956) 1008.
25) S.Chikazumi: AIP Conf. Proc. 29 (1975) 382.
26) S.M.Shapiro, M.Iizumi and G.Shirane: Phys. Rev. B14 (1976) 200.
27) K.Chiba, K.Suzuki and S.Chikazumi: J. Phys. Soc. Jpn. 39 (1975) 839.
28) K.Siratori: unpublished.

CHAPTER 4 SUMMARY

Magnetoelectic effect was investigated for two materials in this thesis. One is antiferromagnetic Cr_2O_3 which have been studied most extensively, and the other is ferrimagnetic Fe_3O_4 below T_v, the low temperature transition point. The effect was quantitatively analyzed especially for the electric field parallel to the c axis in the former case and the crystal symmetry at 77 K was determined and the part of the magnetocrystalline anisotropy, which is accompanied by the electric polarization, was estimated in the latter case.

In Chap. 2, studies on the ME effect of Cr_2O_3 is reported. ME susceptibility (α) was measured carefully and precisely by a SQUID magnetometer, and electric field effect on the antiferromagnetic resonance (AFMR) was examined and the shift was observed at 4.2 K to clarify the mechanism of the ME effect.

On the measurement of α, results are summarized as follows:

1) The linearity of the effect and the sign of α was directly determined. When parallel ME cooling is adopted along the c axis, $\alpha_{//}$ in the high temperature region is positive whereas $\alpha_{//}$ in the low temperature region and $\alpha_{\perp}$ are negative.

2) The characteristic values of α are determined as follows:

$\alpha_{//max} = 23. \times 10^{-6}$ (cgs/g)

$T_{max} = 255$ K

$\alpha_{//4.2K} = 1.2 \times 10^{-6}$ (cgs/g)

$T_{\alpha=0} = 87$ K

$\alpha_{\perp 4.2K} = 7. \times 10^{-6}$ (cgs/g)

3) The temperature dependence of α is similar to that of previous reports, though the values are larger than those previously reported except for the case of $\alpha_{//4.2K}$, data of Mercier in this case was suspected to be due to the setting errors of the crystal.

4) $\alpha_{\perp 4.2K}$ is about 5 times larger than the value of Astrov. ME cooling along the $\underline{c}$ axis probably made this difference. Tilting of the spin axis, which explain the value of $\alpha_{\perp}$, is 3×10^{-3} radian/kV/cm if $S = 3\ \mu_B/Cr^{3+}$ is assumed.

5) If the tilting of the spin axis is due to the tilting of the principal axis of the one-ion anisotropy, that is 200 times larger than that of Cr^{3+} in ruby.

6) $\alpha_{\parallel}$ at 4.2 K gives the value of δg on the assumption that $\delta S = 0$:

$$|\delta g| = 3.5 \times 10^{-8} \qquad \text{at } E = 1 \text{ kV/cm.}$$

7) An extraordinary effect was found in one crystal.

Electric shift in AFMR of Cr_2O_3 at 24.2 GHz was successfully observed at 4.2 K for the first time by the use of ac electric field modulation. The sign of the electric shift was inverted by the inversion of the direction of ME cooling. Results were as follows.

8) The electric shift for the low frequency mode is megative when parallel ME cooling is applied along the $\underline{c}$ axis: the AFMR frequency is lowered if the electric field is applied parallel to the magnetic field.

9) On the sign and the magnitude of the electric shift, contributions of mechanisms of parallel ME effect in Cr_2O_3 were separated experimentally. Assuming $\delta S = 0$ and using the value of δg given

above 6), δD is deduced as

$$\delta D = -1.1 \times 10^{-6} \quad \text{cm}^{-1} \quad \text{at } E = 1 \text{ kV/cm}.$$

This magnitude is only one tenth of that on ruby.

10) Not only the magnitude but also the sign of δD can not explain $\alpha_{//}$ in high temperature region.

Studies on Fe_3O_4 are reported in Chap. 3.

11) The crystal symmetry at 77 K was determined to be " 1 ". However,

12) Breaking of the mirror symmetry parallel to the b plane was much smaller than that of inversion or two-fold rotation parallel to the b axis.

13) ME poling is effective to make the crystal detwinned: Fe_3O_4 is ferroelectric at 77 K.

14) A Richter type relaxation was discovered in the ME effect. The relaxation time is 2 μs at 77 K. This seems to originate from electric relaxation.

15) Magnetic field dependence in the electric susceptibility was observed. ε measured at 100 kHz is about 200 at 77 K.

16) The signal of the ME effect was separated to the rotation and the non-rotation terms, by changing the strength and direction of the external magnetic field. Parameters expressing the rotation term were determined for the external electric field parallel to $[1\bar{1}0]$ and $[11\bar{2}]$ axes. The magnitudes are up to the order of 500 $\text{erg/cm}^3\text{/kV/cm}$.

17) The magnetic anisotropy accompanied by the electric polarization was deduced from the anisotropy of the ME effect. Two

possible directions of the electric polarization were estimated from the rotation of the coordinate and from the principal axis of the anisotropy. This part of the magnetic anisotropy energy is much smaller than the net anisotropy energy.

ACKNOWLEDGEMENTS

The author would like to express his sincere thanks to Professor A. Tasaki of University of Tsukuba and Dr. K. Siratori of Osaka University for their continuous guidances and encouragements throughout this study. Stimulating discussions with Professor K. Kohn of Waseda University is also deeply appreciated. The author is grateful to Professor E. Fujita for critical reading of the manuscript.

The author is indebted to Dr. H. Yasuoka of the Institute for Solid State Physics for supplying a Cr_2O_3 single crystal and to Dr. S. Kimura of National Institute for Researches in Inorganic Materials for supplying Fe_3O_4 single crystals and the annealing of Cr_2O_3 specimens. He also thanks to Dr. H. Hori for the helpful suggestion for the microwave study. Thanks are also due to Professor S. Chikazumi and Dr. H. Miyajima for their hospitality in the experiment using 15 t magnet of the Institute for Solid State Physics. The author is much indebted to Dr. S. Uemura on the measurement of the electric susceptibility and to Dr. M. Mori and Professor Y. Yamada on the X-ray diffraction.

Thanks are also due to Messrs. R. Suzuki and T. Ichihashi for their help in the experiment.